applications, and substantiate that these cell lines are a useful model for understanding the mechanisms of chromosomal instability and differentiation of hMSCs.

Keywords Human cord blood mesenchymal stem cell · Long-term culture · Karyotype analysis · mFISH CGH · Differentiation

Introduction

Tissue-specific stem cells in various adult tissues are known to be an important source in the regeneration of damaged tissue and maintenance of homeostasis in the tissues in which they reside. Among these stem cells, human mesenchymal stem cell (hMSC) has recently become of great interest in regenerative medicine, not only to replenish their own tissues, but also to give rise to more committed progenitor cells, which can differentiate into other tissues. MSCs in bone marrow have been shown to differentiate into several types of cell such as osteoblasts, adipocytes, chondrocytes, myocytes, and probably also neuronal cells (Okamoto et al. 2002; Takeda et al. 2004; Mori et al. 2005; Saito et al. 2005; Terai et al. 2005). Because of these properties, it is expected that hMSCs are an enormous potential source for future cell therapy. The goal of our study is to establish cell lines with long lifespan and with parental properties for clinical application. However, clinical application using these cells has been met with enormous difficulty, e.g., isolation of a cell population with specific criteria, expansion in vitro system for obtaining a sufficient number of cells without affecting their genomic characteristics and differentiation properties, and their storage in higher viability.

At present, there is a little evidence suggesting whether changes in these properties occur during expansion. Human normal MSCs have a limited capacity to replicate in the 40- to 50-population doubling level (PDL) at the most. To extend their lifespan, we have previously established human mesenchymal cell lines from human umbilical cord blood or bone marrow by immortalization with human telomerase reverse transcriptase (hTERT), human papillomavirus high-risk type 16 E6/E7 genes (HPV16E6/E7) or polycomb gene, Bmi-1 (Takeda et al. 2004; Mori et al. 2005; Terai et al. 2005).

hTERT-immortalization without affecting biological characteristics, despite extensive proliferation, has been reported in bone-marrow-derived hMSCs (Burns et al. 2005), human fibroblast (Milyavsky et al. 2003), and human keratinocyte (Harada et al. 2003), although it has been indicated that there is the possibility that prolonged culture of hTERT-immortalized fibroblasts may favor the appearance of clones carrying potentially malignant alterations (Milyavsky et al. 2003). HPV16, which encodes oncogenes (E6 and E7), can also immortalize hMSCs in vitro. Both E6 and E7 proteins act through their association with tumor suppressor gene products, p53 and retinoblastoma family members (pRb), respectively. E6 accelerates the degradation of the p53 protein, which is essential for cell arrest at the checkpoint in G_1/S and at the mitotic checkpoint when tetraploidy occurs (Cross et al. 1995), as well as at the G_2 phase under damaging conditions. E7 protein binds to pRb and abrogates the repressive function of these cell cycle regulations (Zheng et al. 2001). Thus, both p53 and pRb play a multitude of important roles in cell-cycle-progression checkpoints as reported in human keratinocytes (Patel et al. 2004), and fibroblasts (Khan et al. 1998). As a consequence, the disruption of the checkpoints that govern accurate cell division leads to abnormal segregation of chromosome and genomic instability, as shown in the cells immortalized with HPV16E6/E7 genes (Duensing et al. 2002).

In this paper, we report on the chromosomal instability and the differentiation activity during prolonged culture (cell expansion) using four mesenchymal stem cell lines. These results indicate that an umbilical cord blood-derived clone immortalized with hTERT (UCBTERT-21) showed normal karyotype for a period of 1 yr, whereas three other cell lines immortalized with HPV16E6/E7 and hTERT or HPV16E6, Bmi-1 and hTERT showed chromosomal instability but maintained the ability to differentiate.

Materials and Methods

Cell culture. Human mesenchymal stem cell lines, UCB TERT-21 (JCRB1107), UCB408E6E7TERT-33 (JCRB1110), UE6E7T-3 (JCRB1136), and UBE6T-6 (JCRB1140) were obtained from the JCRB Cell Bank (Osaka, Japan). Two of them are cell lines obtained by immortalizing human umbilical cord blood mesenchymal stem cells (UCB) with hTERT alone (UCBTERT-21; Terai et al. 2005) or with HPV16E6/E7 in combination with hTERT (UCB408E6E7TERT-33; Terai et al. 2005), and the two others are human bone-marrow-derived mesenchymal stem cell lines transformed with HPV16E6/E7 and hTERT genes (UE6E7T-3; Mori et al. 2005) or with bmi-1, HPV16E6 and hTERT genes (UBE6T-6; Takeda et al. 2004; Mori et al. 2005).

The UCBTERT-21 and UCB408E6E7TERT-33 were grown in PLUSOID-M medium (Med-Shirotori Co., Tokyo, Japan) or MSCGM BulletKit (Cambrex Co., East Rutherford, NJ). UE6E7T-3 and UBE6T-6 were cultured in POWEREDBY10 medium (Med-Shirotori Co.) or MSCGM BulletKit (Cambrex Co.); 5×10^3 cells/ml of each cell line were seeded and cultured for 7–10 d. When culture

plate was subconfluent, cells were treated with 0.25% trypsin/0.5 mM EDTA solution (both from Invitrogen, Tokyo, Japan) and replated at a density of 5×10^3 cells/ml.

All of the cells were maintained in a humidified incubator at 37° C and 5% CO_2. PDLs were calculated using the formula: PDL= log (cell output/input)/log2. At the starting cultivation, PDLs of UCBTERT-21, UCB408E6E7 TERT-33, UE6E7T-3, and UBE6T-6 were 42, 67, 60, and 56, respectively. The doubling time of the UCB408E6E7T-33 cell was 1.5 d, and that of UCBTERT-21, UE6E7T-3, or UBE6T-6 was 2.6, 2.0, or 4.0 days, respectively.

Measurement of chromosome number and fluorescence in situ hybridization. Metaphase chromosome spreads for measurement of chromosome number and fluorescence in situ hybridization (FISH) were prepared from exponential growing cells at various PDL. The cells were treated in a hypotonic solution after exposure to 0.06 μg/ml colcemid (Invitrogen, Carlsbad, CA) for 2 h and fixed in methanol/acetic acid (3:1). The cells were spread on a microscope slide.

To count the number of chromosomes, the cells were stained with DAPI (4′-6-diaminido-2-phenylindol; Vector Laboratories, Inc. Burlingame, CA) and examined under an Axioplan II imaging microscope (Carl Zeiss, GmbH) equipped with Leica QFISH software (Leica Microsystems Holding, UK). To examine statistically significant chromosome numbers, we have allowed ±1 deviation and 50–100 metaphase spreads were scored for each assay.

Painting probes specific for chromosome 13 (XCP13-kit, FITC; MetaSystems, GmbH) and chromosome 17 (XCP17-kit; Texas Red) (MetaSystems GmbH, Altlussheim, Germany), and multicolor probes (mFISH-24Xcyte-kit, DAPI, FITC, TexasRed, Cy3, Cy5, and DEAC; MetaSystems GmbH) were used for FISH analysis. FISH was performed according to the manufacture's protocol (MetaSystems GmbH). Briefly, both the metaphase chromosome spread and the probe were denatured with 0.07 N NaOH or 70% formamide, hybridized at 37° C for 1–4 d, and counterstained with DAPI. FISH images were captured and analyzed on the Zeiss Axio Imaging microscope (Carl Zeiss Microimaging GmbH, Jena, Germany) with Isis mBAND/mFISH imaging Software (MetaSystems GmbH).

CGH analysis. Hybridization was carried out with the BAC Array (MAC ArrayTM Karyo 4000 Component, Macrogen Co., Rockville, MD) by the Hybstation (Genomic Solutions, Ann Arbor, MI). Briefly, test DNAs, which were isolated using an isolation kit (Amersham BioSciences, Little Chalfont, UK) and Spin Column (QIAGEN Co., Tokyo, Japan), and reference DNAs (Promega Co., Madison, WI), were labeled, respectively, with Cy3 or Cy5 (BioPrimer DNA Labeling System, Invitrogen Co.), precipitated together with ethanol in the presence of Cot-1 DNA, redissolved in a hybridization mixture (50% formamide, 10% dextran sulfate, 2xSSC, 4% sodium dodecyl sulfate [SDS], pH 7), and denatured at 75° C for 10 min. After incubation at 37° C for 30 min, each mixture was applied to an array slide and incubated at 42° C for 48–72 h. After hybridization, the slides were washed in a solution of 50% formamide—2× SSC (pH 7.0) for 15 min at 50° C, in 2× SSC—0.1% SDS for 15 min at 50° C, and in a 100-mM sodium phosphate buffer containing 0.1% Nonidet P-40 (pH 8) for 15 min at room temperature, then scanned with GenePix4000A (Axon Instruments, Union City, CA). Acquired images were analyzed with MacViewer (Macrogen Instruments).

Differentiation ability. To evaluate the differentiation potential of each cell line, cells were cultured on a coverslip in each induction medium, that is, hMSC Differentiation BulletKit-Adipogenic (PT-3004, Cambrex BioScience, Inc., Walkersville, MD) for adipocyte and NPMM Bullet kit (NPMM™ BulletKit (B3209, Cambrex BioScience) for neural progenitor cells. For osteoblast, cells were treated with 0.1 μM dexamethasone (Sigma Chemical Co., St. Louis, MO), 50 μg/ml L-ascorbic acid (Sigma Chemical), and 10 mM β-glycerophosphate (Sigma Chemical) in the PLUSOID-M medium (Med-Shirotori Co.) or the POWER-EDBY10 medium (Med-Shirotori Co.) of culture medium.

After 2–4 wk, the cells were washed in phosphate-buffered saline (PBS), fixed in 4% paraformaldehyde in PBS and stained with Oil Red-O (Sigma Chemical) for detection of adipocyte, and with alkaline phosphatase staining solution containing 0.25 mg/ml naphthol AS-BI phosphate and 0.25 mg/ml Fast violet LB salt for detection of alkaline phosphatase-positive osteoblast. In immunostaining for neuron-like cells, the cells fixed with paraformaldehyde were permeabilized with methanol at −20° C for 10 min and stained with an anti-IIIβ tubulin antibody (Sigma Chemical) or anti-neurofilament antibody NF-200 (Sigma Chemical) and Texas Red-anti-mouse IgG (Southern Biotechnology Associates, Inc., Birmingham, AL) as previously described (Takeuchi et al. 1990).

Results

Changes in chromosomal number in human mesenchymal stem cell lines in prolonged culture. Immortalization of cultured cells frequently induces an abnormal chromosome number as shown in cancer cells (Duensing et al. 2000; Munger et al. 2004; Patel et al. 2004), especially at higher frequency in long-term culture. We therefore examined four cell lines, human mesenchymal stem cell (hMSC) lines immortalized with combinations of bmi-1, E6, E7, and/or hTERT genes, for chromosome instability by counting metaphase chromosomes.

All of the lines were diploid, each containing 46 up to 40 PDL including the PDL numbers of nontransfecting original MSCs (Takeda et al. 2004; Mori et al. 2005; Terai et al. 2005). For UCBTERT-21 cell, no further changes in chromosome number have been observed up to date (for PDL 133) as shown in Fig. 1*A* and *B*. In contrast, although the UBE6T-6 cell and the UE6E7T-3 cell were near diploid, both cells exhibited considerable variation in chromosome number from PDL 70 after the culture started. For example, when the assay of UE6E7T-3 cells start at PDL 62 in culture, 90% of cell population had 46 chromosomes, but the population decreased with prolonged culturing and a population containing 44 chromosomes became dominant (43% of cell populations) at PDL 147 (Fig. 1*E*, *F*). A similar variation was also observed in UBE6T-6 cells (Fig. 1*C*, *D*).

To ascertain whether or not the changes observed were induced by transfection with HPV16E6E7, we assayed the chromosome numbers of UCB408E6E7TERT-33 cell in prolonged culture. The cell line showed similar chromosomal changes to those of the UE6E7T-3 cell, the rate of which was more rapid. At day 2 after culture by us changes became evident (PDL 68), the UCB408E6E7TERT-33 cells consisted of two distinct populations concerning chromosome number (near diploid [24%] and near tetraploid [53%]), shown in Fig. 1*G*. However, the near diploid population was unstable and decreased gradually. At PDL 81, the population became only near tetraploid, 80% of the

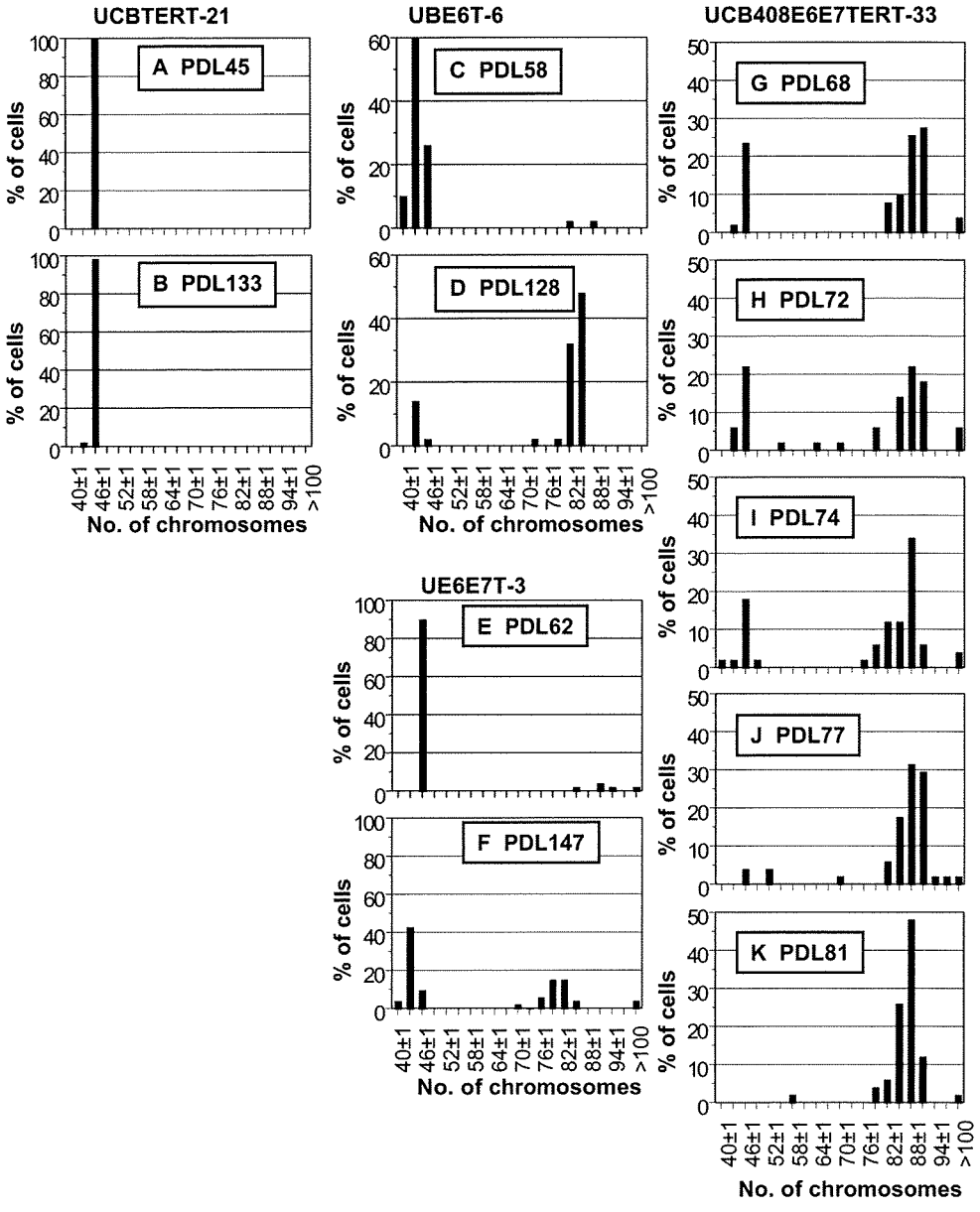

Figure 1. Changes in chromosomal numbers in prolonged cultures of four hMSC cell lines. (*A–K*) The chromosomal numbers at various culture stages were counted by DAPI staining. (*A*, *B*), (*C*, *D*), (*E*, *F*), and (*G–K*) represent the chromosomal numbers from UCBTERT-21, UBE6T-6, UE6E7T-3, and UCB408E6E7TERT-33, respectively. To examine statistically significant chromosomal numbers, we have allowed ±1 deviation, and 50–100 metaphase spreads were examined for each assay. *Note* the changes in chromosomal number from near 2*n* to near 4*n* in prolonged culture.

cells contain 85–92 chromosomes (Fig. 1*K*). The results indicate that UCBTERT-21 is relatively stable in chromosome number, whereas each of the oncogene-immortalized cells (UE6E7T-3, UBE6T-6, and UCB408E6E7TERT-33 cell) were unstable in chromosome numbers, which altered substantially during prolonged culture.

We next applied FISH and CGH analysis to characterize the chromosomal aberrations of the cell lines. All of the four cell lines passed for PDL 50 before examination by FISH. mFISH analysis of the UCBTERT-21 cell at PDL 52 showed normal chromosome composition (Fig. 2*A* and *B*) as observed in non-immortalized cells. The UBE6T-6 cell containing 43–45 chromosomes demonstrates losses of chromosome 13, 16, and 19 (marginal variation in chromosome 4 was observed among cells), but keeps on proliferating in chromosome number of 43–45 (Fig. 2*D*, *E*). In contrast, the UCB408E6E7TERT-33 cell showed more heterogeneity in chromosome composition with intrachromosomal and interchromosomal aberrations (data not shown). However, by mFISH analysis we were able to detect nonrandom losses of chromosome 13 in three cell lines except the UCBTERT-21 cell line. This was also confirmed by pFISH analysis using the probes specific for chromosome 13 and chromosome 17 (Fig. 2*C*, *F*). More than 97% of UCBTERT-21 cells showed two copies for chromosome 13, indicating the stability of the chromosomes in the cell line (Fig. 2*G*). The UE6E7T-3 and the UBE6T-6 cell lines with chromosome numbers of 43–45 showed only one copy of chromosome 13 in 76% of UE6E7T-3 cells and 86% of UBE6T-6 cells, respectively (Fig. 2*I*, *J*). A similar loss of chromosome 13 was also observed in 70% of UCB408E6E7TERT-33 cells, which showed three copies of chromosome 13 in near tetraploid (Fig. 2*H*). Other chromosomes, for example chromosome 17, were contained in the UCBTERT-21 and UBE6T-6 cell lines (Fig. 2*C*, *F*).

Furthermore, a significant nonrandom loss of chromosome 13 at the single cell-level observed by FISH was examined by array CGH, which samples the entire cell population. Figure 3 shows the array CGH profiles from early (*blue spots*) and late (*red spots*) stages of proliferating of each cell line. The UCBTERT-21 cell did not show any detectable differences in array CGH profiles between early and late stages (Fig. 3*A*). Although the loss of chromosome 13 had already occurred at early stages in the UBE6T-6 and the UCB408E6E7TERT-33 cell lines, in addition to the losses of chromosomes 4, 9, and 16 (Fig. 3*B*, *D*), in UE6E7T-3 the loss appeared between PDL 78 to 101 with loss of chromosome 16. The most compelling observation was that all three cell lines revealed a consistent whole loss of chromosome 13. These data are consistent with the results observed by FISH analysis. From these results, we

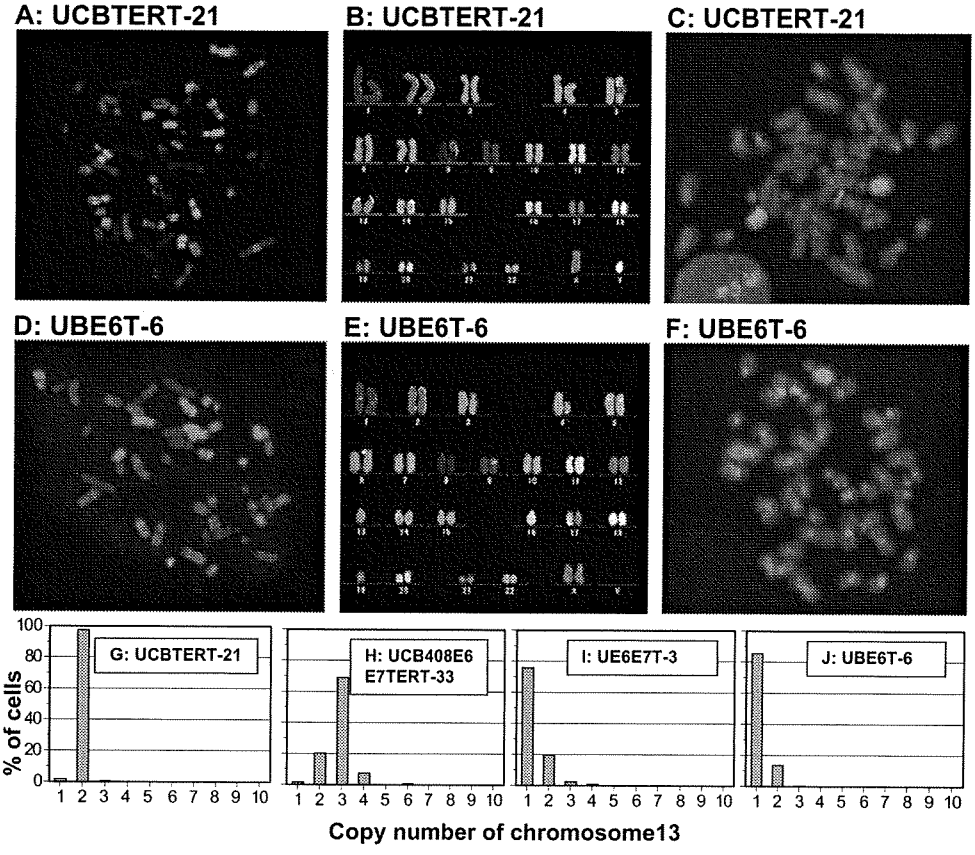

Figure 2. FISH analysis of human mesenchymal stem cell (hMSC) lines immortalized with hTERT alone, hTERT plus bm-1, HPVE6 or with hTERT plus HPVE6/E7. Multicolor FISH images of metaphase spreads (*A*, *D*), their karyotypes (*B*, *E*), and painting FISH images using DNA probes specific for chromosome 13 (*green*) and 17 (*red*) (*C*, *F*) of UCBTERT-21 (*A*, *B*, *C*) and UBE6T-6 (*D*, *E*, *F*). Quantity of chromosome 13 copy numbers in four cell lines (*G–J*). FISH signals were counted in 120~200 metaphase spreads plus interphase nuclei. UCBTERT-21 cells contained two copies of chromosome 13 and 17, and showed normal human karyotype, whereas other cells lost one copy of chromosome 13.

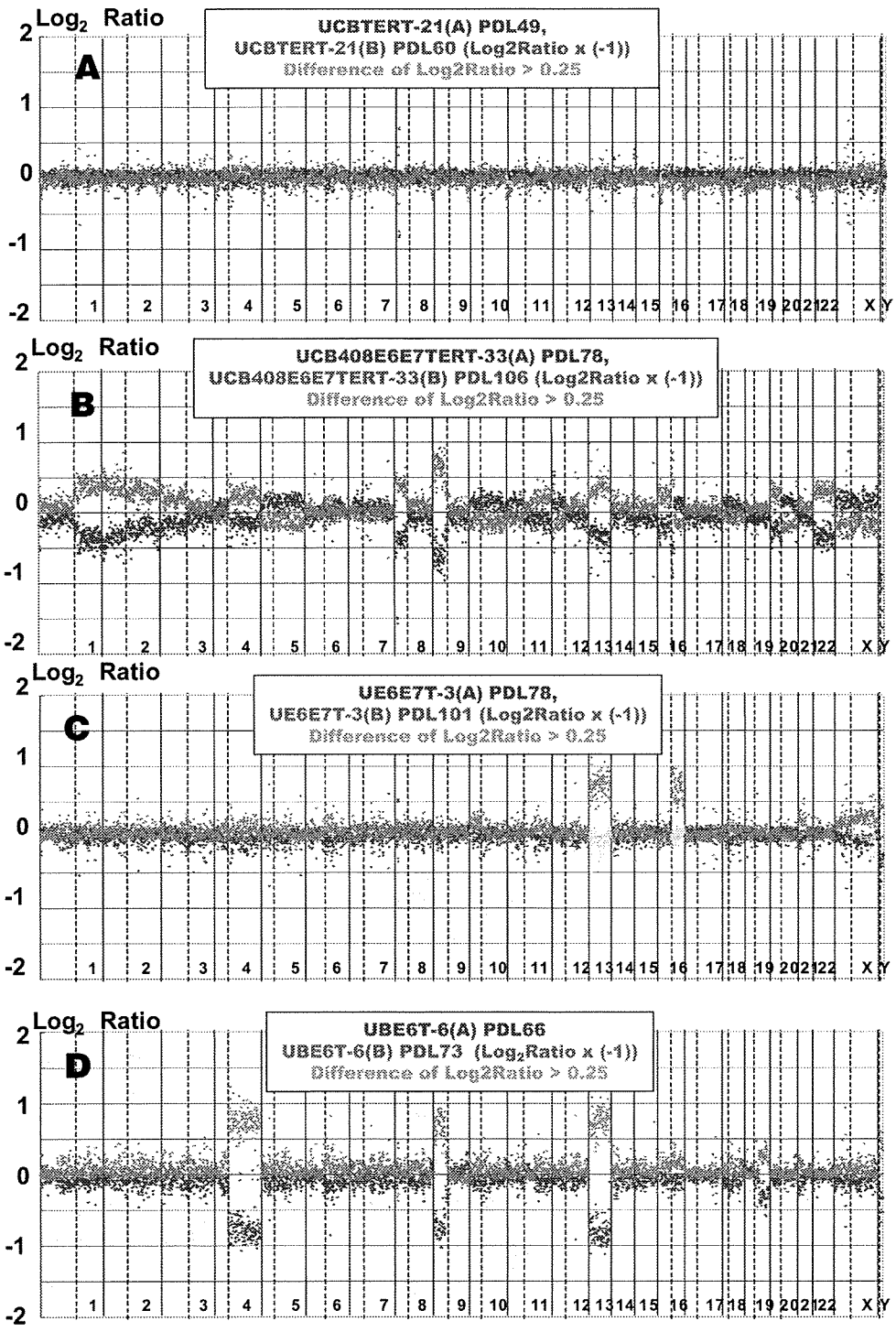

Figure 3. Array CGH profiles performed on four immortalized human mesenchymal stem cell lines at selected PDL. For each *panel*, the *X*-axis represents the 22 autosomes, the *X* and *Y* chromosomes, and the *Y*-axis shows the $\log_2$ of the fluorescence intensity ratio (cy3 [hMSCs]/cy5 [normal cell]) of all spots of the chromosome. Values above 0 (*red spots*) or values below 0 (*blue spots*) signify a loss of chromosome (chromosome regions). *Blue spots* in each *panel* indicate the $\log_2$ ratios observed at early stage in the culture of each cell line, which are overlaid with *red spots* indicated at the late stage. *Green spots* indicate the difference in value between *blue spots* and *red spot*. *Note* that in the UE6E7T-3 cell line, one copy of chromosome 13 and 16 were lost between PDL 78 and 101.

concluded that only hTERT-mediated immortalization induced little change in the chromosome numbers and chromosome structures of mesenchymal stem cells, but immortalization with Bmi-1, E6, and E7 in addition to hTERT results in chromosome instability.

Differentiation potential into lineages of immortalized mesenchymal stem cell lines. It has been reported that mesenchymal stem cells have the extensive potential to differentiate into multiple cell lineages including osteoblast, chondrocytes, adipocytes (Pittenger et al. 1999), cardiac myocytes (Makino et al. 1999), and neural cells (Pacary et al. 2006; Wislet-Gendebien et al. 2005). To evaluate whether chromosome instability of these cell lines in prolonged culture affects differentiation, cells of each cell line were stimulated in each induction medium for 2 to 4 wk. In

adipocyte-specific culture medium, all cell lines accumulated lipid-rich vacuoles in their cytoplasm within 2 wk, which were made evident by Oil Red-O staining. In particular, the UE6E7T-3 cell line showed a greater adipogenetic ability among the four cell lines (Fig. 4*Ab*). In osteoblast induction medium for 2 wk, UCB408E6E7 TERT-33 cells showed a marked increase in alkaline phosphatase expression, a marker of osteoblast, compared with those in the three other cell lines (Fig. 4*Ad*). In addition, UBE6T-6 cells in neuron induction medium reduced proliferation and displayed marked changes in morphology from being a flat-polygonal shape to taking on the characteristic neuron-like shape in which the cells develop long branching processes. Moreover, in comparing the expression patterns of characteristic neural antigens, i.e., neurofilament, III-β-tubulin, before and after induction (28 d), the pseudo-neural shaped cells showed apparent increases in immunoreactivity to both antibodies (Fig. 4*Af, Ah*),

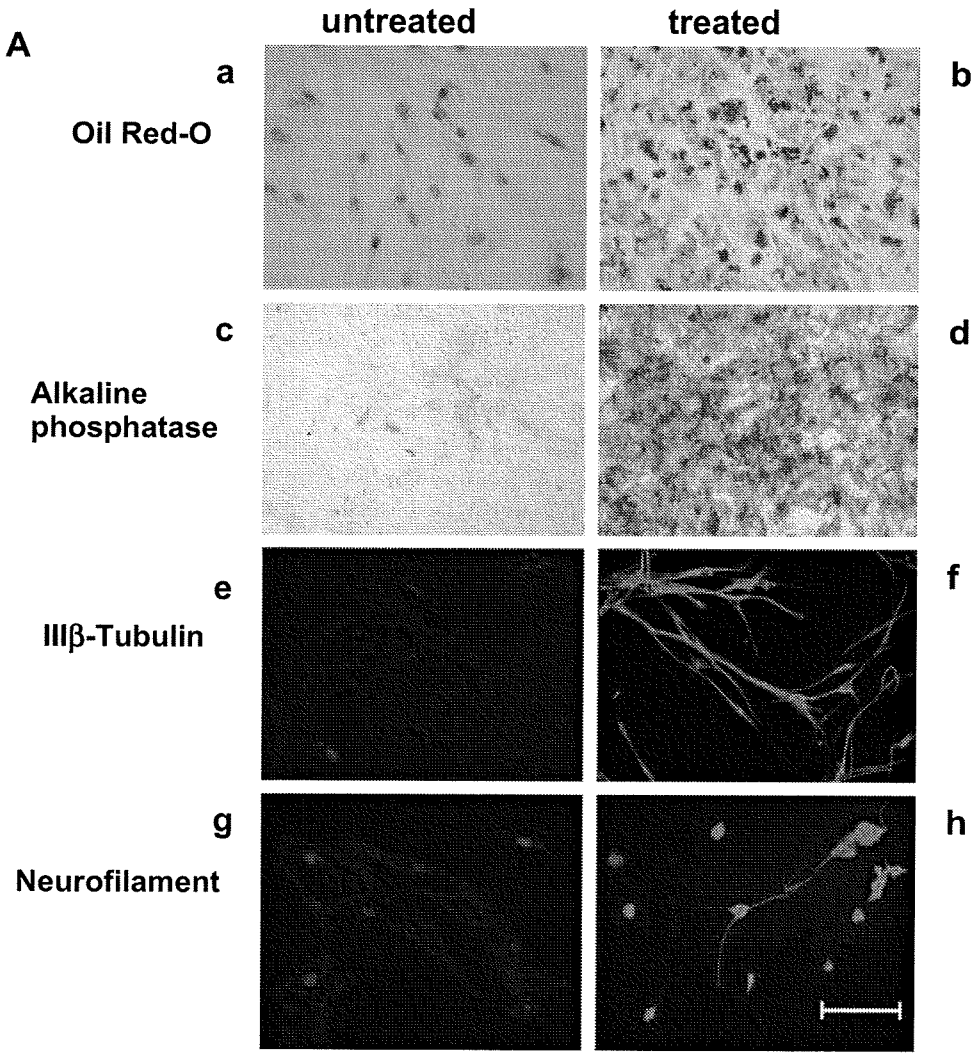

Figure 4. Differentiation potential of immortalized human mesenchymal stem cell lines into adipogenic, osteogenic, and neurogenic lineages. Adipogenesis was indicated by the accumulation of lipid stained with Oil Red-O (*Aa* and *Ab*, UE6E7T-3 cell line). Osteogenesis is indicated by the increase in alkaline phosphatase (*Ac* and *Ad*, UCB408E6E7TERT-33 cell line). Neurogenesis was shown by staining with two kinds of monoclonal antibodies to IIIβ-tubulin and neurofilament, and by shape changes of cell (*Ae–Ah*, UBE6T-6 cell line). *B*, Comparison of the differentiation potential of four cell lines whose responses to stimuli into differentiation were diverse among the cell lines. − and + indicate a response similar to an untreated cell and a weak positive response. +++ indicates a strong response shown by images of treated cells in Fig. 4*A*. (*Bar* indicates 20 μm).

B

	UCBTERT-21	UCB408E6E7TERT-33	UE6E7T-3	UBE6T-6
Oil Red-O	+	++	+++	+
Alkarine phosphatase	+	+++	+	+
IIIβ- Tubulin	-	+	+/-	+++
Neurofilament	-	++	-	++

whereas such changes were not evident with the flat-shaped cells before induction (Fig. 4*Ae*, *Ag*). Additionally, such cells did not undergo such differentiation in culture medium when cultured for as long as 30 d, although faint staining was observed. Figure 4*B* shows the overall results of differentiation potential of the four cell lines into adipogenic, osteogenic, and neurogenic lineages. These immortalized mesenchymal stem cell lines retained the ability to differentiate into three lineages, although among cell lines there are significant variations in response to lineage-specific induction.

Discussion

Attempts to clarify the mechanisms for extending the lifespan of tumor cells have been made for many years, and several genes that have effects on cellular proliferation and survival have become clear (Munger et al. 2002) in addition to the elucidation that the majority of tumor cells express telomerase (hTERT; Armanios et al. 2005). The goal of one of the series of our studies has been to establish cell lines with long lifespan and with parental properties, on the basis of genotypic and phenotypic characterizations, for application to cell-based therapy. We previously established several cell lines (Takeda et al. 2004; Mori et al. 2005; Terai et al. 2005), and the present study demonstrated that UCBTERT-21, the immortalized cell line derived from human umbilical cord blood-derived MSCs with hTERT, has a normal karyotype and has an extended lifespan by at least 133 population doublings, and has the differentiation potential into the adipocyte or osteoblast similar to parental MSCs (Terai et al. 2005), although the potential was weak but clearly positive in this study. The specific environmental cues to initiate the differentiation of hMSCs are not yet clear.

UCBTERT-21 immortalized with hTERT alone can be prolonged without inhibition of the $p16^{INK4A}$/RB pathway (Terai et al. 2005), the result of which is in agreement with reports that hTERT alone significantly extends the lifespan of human fibroblasts, epithelial, and endothelial cells (Bodnar et al. 1998; Chang et al. 2005), without the requirement for molecular alterations in p53/p21 and pRB/$p16^{INK4A}$ pathways (Milyavsky et al. 2003). However, other researchers have indicated that inactivation of the RB/p16 pathway by E7, or downregulation of p16 expression, in addition to increasing telomerase activities, is necessary for expanding the lifespan of human keratinocytes (Dickson et al. 2000; Kiyono et al. 1998). Thus, the possibility that a telomere-independent barrier may operate to prevent immortalization according to cell types has been indicated.

UCB408E6E7TERT-33, UE6E7T-3, and UBE6T-6 are hMSC-clones immortalized with HPV16E6/E7 or polycomb group oncogene Bmi-1, in combination with hTERT. Immortalization of human keratinocyte in vitro using virus-derived oncogenes such as E6 and E7 is based on initial inactivation of the p53 and/or Rb pathways, which are essential for controlling cell cycle progression in response to DNA damage or after induction tetraploidy; therefore, this gene transduction induces chromosomal abnormalities (Solinas-Toldo et al. 1997; Duensing et al. 2002; Patel et al. 2004; Schaeffer et al. 2004). The cell lines used in this study became completely immortal, yet underwent dynamic changes in their chromosome numbers in prolonged culture. Near diploid population in early passage of UCB408E6E7 TERT-33 became near-tetraploid population with prolonged culture without the appearance of intermediate populations (60–70 chromosomes/cell), and thereafter gave rise to a population having smaller numbers of chromosomes than tetraploid. Similar patterns existed, although at a slower rate, in UBE6T-6 cells and UE6E7T-3. These results suggest that HPVE6 and E7 proteins cause tetraploidy that precedes the chromosomal aberration to aneuploid in E6/E7-immotalized hMSCs, as is currently shown in several lines of evidence. For example, in vitro experiments in human cell lines (N/TERT-1 keratinocytes and HeLa cells) demonstrate that chromosome nondisjunction yields tetraploid rather than aneuploid, and that aneuploid may develop through chromosomal loss from tetraploid, although the mechanistic basis for the tetraploid formation still remains to be elucidated (Shi et al. 2005). This is also suggested from evidence that high frequency of tetraproidy is present with aneuploidy in human tumors (Olaharski et al. 2006; Sen 2000). A distinct pattern of aneuploid became apparent using dual-probe FISH and CGH analyses, in which UCB408E6E7TERT-33 cells predominantly exhibited triploid 13 and tetraploidy 17 together with other chromosomal changes as shown in Figs. 2 and 3. However, surprisingly, the loss of one copy of chromosome 13 was also seen in 70–80% of diploid UE6E7T-3 and diploid UBE6T-6 cells retaining two copies of chromosome 17. The loss occurred in PDL 50 in both UE6E7T-6 and UCB408E6E7TERT-33, and between PDL 78 and 101 in UE6E7T-3. Structural and numerical aberrations targeting chromosome 17 are often reported in tumors from various tissues (Olaharski et al. 2006), whereas the pattern that chromosome 13 is lost and chromosome 17 is stable, was common for the three cell lines in this study, indicating the possibility that the loss of chromosome 13 may play an important role in the chromosomal aberration of hMSCs to acquire growth advantages under the given culturing condition. Similar karyotypic changes were evident in cultured human embryonic stem cells, involving the gain of chromosome 17 or chromosome 12 (Carlson et al. 2000; Draper et al. 2004). It is thus conjectured that the aneuploidy developed through chromosomal loss from

diploid cells arises through different mechanisms from tetraploid intermediate.

An alternative explanation for aneuploid formation mechanism independent of tetraploid intermediate is loss of regulation in centrosome duplication, leading to abnormal centrosome amplification and multipolar spindles, resulting in aneuploidy. In addition, centrosome amplification caused by loss of p53 has been shown in cultured mouse cells (Fukasawa et al. 1996), but not in cultured human cells (Kawamura et al. 2004). However, loss of p53 and centrosome amplification has been revealed in human cancer tissue. Our preliminary examination has indicated a weak correlation between centrosome amplification and chromosome number (data not shown). Only 2.4% of UCBTERT-21 cells contained >3 centrosomes per cell, whereas 11.9% of UCB408E6E7TERT-33, 19.1% of UE6E7T-3 and 14.3% of UBE6T-6 cells contained >3 centrosomes per cell. Thus, further study is still needed to clarify the mechanism inducing chromosomal instability in immortalized hMSCs cultured over a long period.

Human mesenchymal stem cells are thought to be multipotent cells that can replicate stem cells and that can differentiate to lineages of mesenchymal tissues including bone, fat, tendon, and muscle. Our results indicated that immortalized hMSCs, except UCBTERT-21, induced changes in chromosome number over prolonged culture, but these cells have still retained the ability to both proliferate and differentiate. Immortalized UBE6T-6 cells also displayed neuron-like morphology and strong expression of the neuron-specific markers of neurofilament and III-β-tubulin. We previously demonstrated that hTERT, E7-immortalized hMSCs differentiate into neural cells in vitro on the basis of morphological changes, expression of neural markers such as nestin, neurofilament, MAP-2, Nurr1, and III-β-tubulin. Furthermore, the physiological function showed reversible calcium uptake in response to extracellular potassium concentration (Mori et al. 2005). Similar observations have been reported using rat MSCs (Wislet-Gendebien et al. 2003; Wislet-Gendebien et al. 2005; Pacary et al. 2006). In preliminary experiment of cell transplantation that 10^6 cells of UCBTERT-21 cell (PDLs 120) or UCB408E6E7TERT-33 cell (PDLs 200) were injected into nude mice subcutaneously, no tumorigenicity was observed (data not shown).

In conclusion, our study showed that the hTERT-immortalized cell line displayed normal karyotype and differentiation ability in prolonged culture. These results provide a step forward toward supplying a sufficient number of cells for new therapeutic approaches. In addition, oncogene-immortalized cell lines exhibited abnormal karyotype accompanying the preferential loss of chromosome 13 but without differential alteration during prolonged culture. Thus, the results could provide a useful model for understanding the mechanisms of the chromosomal instability and the differentiation of hMSC.

Acknowledgments This study was supported in part by a grant from the Ministry of Health, Labor and Welfare of Japan. We are grateful to Dr. T.Masui for his advice on ethics problems, and to Mr. H.Migitaka (Carl Zeiss Co., Ltd.) for his assistance with mFISH karyotype analysis. M.T. and K.T. contributed equally to this work.

References

Armanios, M.; Greider, C. W. Telomerase and cancer stem cells. Cold Spring Harbor Symp. Quant. Biol. 70:205–208; 2005.

Bodnar, A. G.; Ouellette, M.; Frolkis, M.; Holt, S. E.; Chiu, C. P.; Morin, G. B.; Harley, C. B.; Shay, J. W.; Lichtsteiner, S.; Wright, W. E. Extension of life-span by introduction of telomerase into normal human cells. Science 279:349–352; 1998.

Burns, J. S.; Abdallah, B. M.; Guldberg, P.; Rygaard, J.; Schroder, H. D.; Kassem, M. Tumorigenic heterogeneity in cancer stem cells evolved from long-term cultures of telomerase-immortalized human mesenchymal stem cells. Cancer Res. 65:3126–3135; 2005.

Carlson, J. A.; Healy, K.; Tran, T. A.; Malfetano, J.; Wilson, V. L.; Rohwedder, A.; Ross, J. S. Chromosome 17 aneusomy detected by fluorescence in situ hybridization in vulvar squamous cell carcinomas and synchronous vulvar skin. Am. J. Pathol. 157:973–983; 2000.

Chang, M. W.; Grillari, J.; Mayrhofer, C.; Fortschegger, K.; Allmaier, G.; Marzban, G.; Katinger, H.; Voglauer, R. Comparison of early passage, senescent and hTERT immortalized endothelial cells. Exp. Cell Res. 309:121–136; 2005.

Cross, S. M.; Sanchez, C. A.; Morgan, C. A.; Schimke, M. K.; Ramel, S.; Idzerda, R. L.; Raskind, W. H.; Reid, B. J. A p53-dependent mouse spindle checkpoint. Science 267:1353–1356; 1995.

Dickson, M. A.; Hahn, W. C.; Ino, Y.; Ronfard, V.; Wu, J. Y.; Weinberg, R. A.; Louis, D. N.; Li, F. P.; Rheinwald, J. G. Human keratinocytes that express hTERT and also bypass a p16(INK4a)-enforced mechanism that limits life span become immortal yet retain normal growth and differentiation characteristics. Mol. Cell Biol. 20:1436–1447; 2000.

Draper, J. S.; Smith, K.; Gokhale, P.; Moore, H. D.; Maltby, E.; Johnson, J.; Meisner, L.; Zwaka, T. P.; Thomson, J. A.; Andrews, P. W. Recurrent gain of chromosomes 17q and 12 in cultured human embryonic stem cells. Nat. Biotechnol. 22:53–54; 2004.

Duensing, S.; Lee, L. Y.; Duensing, A.; Basile, J.; Piboonniyom, S.; Gonzalez, S.; Crum, C. P.; Munger, K. The human papillomavirus type 16 E6 and E7 oncoproteins cooperate to induce mitotic defects and genomic instability by uncoupling centrosome duplication from the cell division cycle. Proc. Natl. Acad.Sci. U. S. A. 97:10002–10007; 2000.

Duensing, S.; Munger, K. The human papillomavirus type 16 E6 and E7 oncoproteins independently induce numerical and structural chromosome instability. Cancer Res. 62:7075–7082; 2002.

Fukasawa, K.; Choi, T.; Kuriyama, R.; Rulong, S.; Vande Woude, G. F. Abnormal centrosome amplification in the absence of p53. Science 271:1744–1747; 1996.

Harada, H.; Nakagawa, H.; Oyama, K.; Takaoka, M.; Andl, C. D.; Jacobmeier, B.; von, W. A.; Enders, G. H.; Opitz, O. G.; Rustgi, A. K. Telomerase induces immortalization of human esophageal keratinocytes without p16INK4a inactivation. Mol. Cancer Res. 1:729–738; 2003.

Kawamura, K.; Izumi, H.; Ma, Z.; Ikeda, R.; Moriyama, M.; Tanaka, T.; Nojima, T.; Levin, L. S.; Fujikawa-Yamamoto, K.; Suzuki, K.; Fukasawa, K. Induction of centrosome amplification and

chromosome instability in human bladder cancer cells by p53 mutation and cyclin E overexpression. Cancer Res. 64:4800–4809; 2004.

Khan, S. H.; Wahl, G. M. p53 and pRb prevent rereplication in response to microtubule inhibitors by mediating a reversible G1 arrest. Cancer Res. 58:396–401; 1998.

Kiyono, T.; Foster, S. A.; Koop, J. I.; McDougall, J. K.; Galloway, D. A.; Klingelhutz, A. J. Both Rb/p16INK4a inactivation and telomerase activity are required to immortalize human epithelial cells. Nature 396:84–88; 1998.

Makino, S.; Fukuda, K.; Miyoshi, S.; Konishi, F.; Kodama, H.; Pan, J.; Sano, M.; Takahashi, T.; Hori, S.; Abe, H.; Hata, J.; Umezawa, A.; Ogawa, S. Cardiomyocytes can be generated from marrow stromal cells in vitro. J. Clin. Invest. 103:697–705; 1999.

Milyavsky, M.; Shats, I.; Erez, N.; Tang, X.; Senderovich, S.; Meerson, A.; Tabach, Y.; Goldfinger, N.; Ginsberg, D.; Harris, C. C.; Rotter, V. Prolonged culture of telomerase-immortalized human fibroblasts leads to a premalignant phenotype. Cancer Res. 63:7147–7157; 2003.

Mori, T.; Kiyono, T.; Imabayashi, H.; Takeda, Y.; Tsuchiya, K.; Miyoshi, S.; Makino, H.; Matsumoto, K.; Saito, H.; Ogawa, S.; Sakamoto, M.; Hata, J.; Umezawa, A. Combination of hTERT and bmi-1, E6, or E7 induces prolongation of the life span of bone marrow stromal cells from an elderly donor without affecting their neurogenic potential. Mol. Cell Biol. 25:5183–5195; 2005.

Munger, K.; Baldwin, A.; Edwards, K. M.; Hayakawa, H.; Nguyen, C. L.; Owens, M.; Grace, M.; Huh, K. Mechanisms of human papillomavirus-induced oncogenesis. J. Virol. 78:11451–11460; 2004.

Munger, K.; Howley, P. M. Human papillomavirus immortalization and transformation functions. Virus Res. 89:213–228; 2002.

Okamoto, T.; Aoyama, T.; Nakayama, T.; Nakamata, T.; Hosaka, T.; Nishijo, K.; Nakamura, T.; Kiyono, T.; Toguchida, J. Clonal heterogeneity in differentiation potential of immortalized human mesenchymal stem cells3. Biochem. Biophys. Res. Commun. 295:354–361; 2002.

Olaharski, A. J.; Sotelo, R.; Solorza-Luna, G.; Gonsebatt, M. E.; Guzman, P.; Mohar, A.; Eastmond, D. A. Tetraploidy and chromosomal instability are early events during cervical carcinogenesis. Carcinogenesis 27:337–343; 2006.

Pacary, E.; Legros, H.; Valable, S.; Duchatelle, P.; Lecocq, M.; Petit, E.; Nicole, O.; Bernaudin, M. Synergistic effects of CoCl(2) and ROCK inhibition on mesenchymal stem cell differentiation into neuron-like cells. J. Cell Sci. 119:2667–2678; 2006.

Patel, D.; Incassati, A.; Wang, N.; McCance, D. J. Human papillomavirus type 16 E6 and E7 cause polyploidy in human keratinocytes and up-regulation of G2-M-phase proteins. Cancer Res. 64:1299–1306; 2004.

Pittenger, M. F.; Mackay, A. M.; Beck, S. C.; Jaiswal, R. K.; Douglas, R.; Mosca, J. D.; Moorman, M. A.; Simonetti, D. W.; Craig, S.; Marshak, D. R. Multilineage potential of adult human mesenchymal stem cells. Science 284:143–147; 1999.

Saito, M.; Handa, K.; Kiyono, T.; Hattori, S.; Yokoi, T.; Tsubakimoto, T.; Harada, H.; Noguchi, T.; Toyoda, M.; Sato, S.; Teranaka, T. Immortalization of cementoblast progenitor cells with Bmi-1 and TERT. J. Bone Miner. Res. 20:50–57; 2005.

Schaeffer, A. J.; Nguyen, M.; Liem, A.; Lee, D.; Montagna, C.; Lambert, P. F.; Ried, T.; Difilippantonio, M. J. E6 and E7 oncoproteins induce distinct patterns of chromosomal aneuploidy in skin tumors from transgenic mice. Cancer Res. 64:538–546; 2004.

Sen, S. Aneuploidy and cancer. Curr. Opin. Oncol. 12:82–88; 2000.

Shi, Q.; King, R. W. Chromosome nondisjunction yields tetraploid rather than aneuploid cells in human cell lines. Nature 437:1038–1042; 2005.

Solinas-Toldo, S.; Durst, M.; Lichter, P. Specific chromosomal imbalances in human papillomavirus-transfected cells during progression toward immortality. Proc. Natl. Acad. Sci. U. S. A 94:3854–3859; 1997.

Takeda, Y.; Mori, T.; Imabayashi, H.; Kiyono, T.; Gojo, S.; Miyoshi, S.; Hida, N.; Ita, M.; Segawa, K.; Ogawa, S.; Sakamoto, M.; Nakamura, S.; Umezawa, A. Can the life span of human marrow stromal cells be prolonged by bmi-1, E6, E7, and/or telomerase without affecting cardiomyogenic differentiation? J. Gene Med. 6:833–845; 2004.

Takeuchi, K.; Kuroda, K.; Ishigami, M.; Nakamura, T. Actin cytoskeleton of resting bovine platelets. Exp. Cell Res. 186:374–380; 1990.

Terai, M.; Uyama, T.; Sugiki, T.; Li, X. K.; Umezawa, A.; Kiyono, T. Immortalization of human fetal cells: the life span of umbilical cord blood-derived cells can be prolonged without manipulating p16INK4a/RB braking pathway. Mol. Biol. Cell 16:1491–1499; 2005.

Wislet-Gendebien, S.; Hans, G.; Leprince, P.; Rigo, J. M.; Moonen, G.; Rogister, B. Plasticity of cultured mesenchymal stem cells: switch from nestin-positive to excitable neuron-like phenotype. Stem Cells 23:392–402; 2005.

Wislet-Gendebien, S.; Leprince, P.; Moonen, G.; Rogister, B. Regulation of neural markers nestin and GFAP expression by cultivated bone marrow stromal cells. J. Cell Sci. 116:3295–3302; 2003.

Zheng, L.; Lee, W. H. The retinoblastoma gene: a prototypic and multifunctional tumor suppressor. Exp. Cell Res. 264:2–18; 2001.

In Vitro Cell.Dev.Biol.—Animal
DOI 10.1007/s11626-009-9266-6

BMP4 induction of trophoblast from mouse embryonic stem cells in defined culture conditions on laminin

Yohei Hayashi · Miho Kusuda Furue · Satoshi Tanaka · Michiko Hirose · Noriko Wakisaka · Hiroki Danno · Kiyoshi Ohnuma · Shiho Oeda · Yuko Aihara · Kunio Shiota · Atsuo Ogura · Shoichi Ishiura · Makoto Asashima

Received: 12 October 2009 / Accepted: 16 November 2009 / Editor: J. Denry Sato

Abstract Because mouse embryonic stem cells (mESCs) do not contribute to the formation of extraembryonic placenta when they are injected into blastocysts, it is believed that mESCs do not differentiate into trophoblast whereas human embryonic stem cells (hESCs) can express trophoblast markers when exposed to bone morphogenetic protein 4 (BMP4) in vitro. To test whether mESCs have the potential to differentiate into trophoblast, we assessed the effect of BMP4 on mESCs in a defined monolayer culture condition. The expression of trophoblast-specific transcription factors such as *Cdx2*, *Dlx3*, *Esx1*, *Gata3*, *Hand1*, *Mash2*, and *Plx1* was specifically upregulated in the BMP4-treated differentiated cells, and these cells expressed trophoblast markers. These results suggest that BMP4 treatment in defined culture conditions enabled mESCs to differentiate into trophoblast. This differentiation was inhibited by serum or leukemia inhibitory factor, which are generally used for mESC culture. In addition, we studied the mechanism underlying BMP4-directed mESC differentiation into trophoblast. Our results showed that BMP4 activates the Smad pathway in mESCs inducing *Cdx2* expression, which plays a crucial role in trophoblast differentiation, through the binding of Smad protein to the *Cdx2* genomic enhancer sequence. Our findings imply that there is a common molecular mechanism underlying hESC and mESC differentiation into trophoblast.

Keywords BMP4 · Smad · *Cdx2* · Trophoblast · Mouse embryonic stem cells

Y. Hayashi · H. Danno · K. Ohnuma · S. Oeda · Y. Aihara · S. Ishiura · M. Asashima
Department of Life Sciences (Biology), Graduate School of Arts and Sciences, The University of Tokyo, Tokyo 153-8902, Japan

S. Tanaka · K. Shiota
Laboratory of Cellular Biochemistry, Animal Resource Sciences/ Veterinary Medical Sciences, The University of Tokyo, Tokyo 113-8657, Japan

M. Hirose · N. Wakisaka · A. Ogura
Bioresource Center, RIKEN, Ibaraki 305-0074, Japan

M. Asashima
Organ Development Research Laboratory, National Institute of Advanced Industrial Science and Technology, Ibaraki 305-8562, Japan

M. K. Furue (✉) · Y. Aihara
Japanese Collection of Research Bioresources (JCRB) Cell Bank, Laboratory of Cell Culture, Division of Bioresources, National Institute of Biomedical Innovation, 7-6-8 Asagi Saito, Ibaraki, Osaka 567-0085, Japan
e-mail: mkfurue@nibio.go.jp

Introduction

Mouse embryonic stem cells (mESCs) are pluripotent cells derived from the inner cell mass (ICM) of the blastocyst, which differentiate into all the three germ layers in vitro and in vivo (Evans and Kaufman 1981; Martin 1981). However, mESCs are thought to be incapable of differentiating into trophoblast because they do not contribute to placenta in chimeric mouse (Beddington and Robertson 1989). To obtain placental trophoblast from mESCs, genetic manipulations of transcription factors or signaling molecules have been reported, such as the decreased expression of *Oct3/4* (Niwa et al. 2000) or *Sox2* (Masui et al. 2007) or overexpression of *Cdx2* (Niwa et al. 2005; Tolkunova et al. 2006), *Eomes* (Niwa et al. 2005), *Ras* (Lu

Published online: 24 December 2009

et al. 2008), or *Tead4* (Nishioka et al. 2009). However, the fundamental molecular mechanisms regulating the differentiation of ESCs into trophoblast have not yet been elucidated. Human embryonic stem cells (hESCs) have been reported to express trophoblast markers after treatment with bone morphogenetic protein 4 (BMP4) in vitro (Xu et al. 2002). By contrast, the effect of BMP4 on mESCs is still unclear (Kunath et al. 2007). BMP4 is thought to be involved in activin- or Wnt-induced mesoderm induction or mesodermal tissue specification from ESCs (Johansson and Wiles 1995; Wiles and Johansson 1999; Nostro et al. 2008; Sumi et al. 2008). Coordinating with leukemia inhibitory factor (LIF), BMP4 also supports the mESC self-renewal in defined culture conditions (Ying et al. 2003; Qi et al. 2004).

Recently, Smith and his colleagues have suggested that to elucidate physiologically relevant molecular signals in mESCs, culture conditions with fewer extrinsic stimulators are beneficial (Ying et al. 2008). We previously developed a chemically defined simple serum-free culture condition for mESCs (Furue et al. 2005). Under these culture conditions, the effects of extracellular matrices (ECM) on mESCs were studied, and the results revealed that laminin promoted differentiation into epiblast-like cells (Hayashi et al. 2007). In this study, we assessed the effect of BMP4 on mESC in the defined culture conditions with fewer extrinsic stimulators. Our results show that mESCs can be induced to differentiate into trophoblast by BMP4 in vitro. This differentiation was inhibited by serum or LIF. Furthermore, we also found that BMP4 activates the Smad pathway in mESCs, and in turn, the BMP–Smad pathway directly induces *Cdx2* expression, which plays a crucial role in trophoblast differentiation.

Materials and Methods

Cell culture. The mESC D3 line (CRL-1934, ATCC, Manassas, VA), B6G-2 line (AES0003, RIKEN Cell Bank, Ibaraki, Japan), E14 line, or EB3 line was routinely cultured in 75-cm^2 plastic flasks (Corning, Corning, NY), coated with 15 μg/ml of type I collagen (Nitta gelatin) in a humidified atmosphere of 5% CO_2 at 37°C in a defined ESF7 medium. The ESF7 consisted of ESF basal medium (Cell Science & Technology Institute, Sendai, Japan) supplemented with 10 μg/ml of insulin, 5 μg/ml transferrin, 10 μM 2-mercaptoethanol, 10 μM 2-ethanolamine, 20 nM sodium selenite, 9.4 μg/ml of oleic acid conjugated with 2 mg/ml of fatty-acid-free bovine serum albumin (FAF-BSA; Sigma, St. Louis, MO), and 10 ng/ml of LIF (Chemicon, Billerica, MA), as described previously (Furue et al. 2005; Hayashi et al. 2007). For the differentiation experiments, mESCs were seeded at a density of 1×10^4 cells per square centimeter in the ESF5 medium comprised of ESF basal medium supplemented with 10 μg/ml of insulin, 5 μg/ml transferrin, 10 μM 2-mercaptoethanol, 10 μM 2-ethanolamine, 20 nM sodium selenite added with 0.5 mg/ml FAF-BSA, and 10 ng/ml rhBMP4 (R&D Systems, Minneapolis, MN) on 2 μg/cm^2 laminin-coated (Sigma) dishes. The medium was changed every 2 d. After 4 d of culture under differentiating conditions, the cells reached confluency. Then, in all experiments where cells were differentiated for more than 4 d, the cells cultured for 4 d in BMP4-supplemented ESF5 medium were harvested with 0.2 mg/ml ethylenediaminetetraacetic acid (EDTA)-4Na (Sigma) for 5 min at room temperature and subcultured into BMP4-supplemented ESF5 medium at a density of about 2×10^4 cells per square centimeter. For the examination of the effects of activin and FGF4 on the differentiation of mESCs into trophoblast, the mESCs were cultured in ESF5 medium supplemented with 25 ng/ml of FGF4 (Sigma) or 10 ng/ml of activin A (Ajinomoto, Kawasaki, Japan), respectively. When examining the effect of fetal calf serum (FCS), LIF, and Noggin on the differentiation of mESCs into trophoblast, the mESCs were cultured in ESF5 medium supplemented with 10 ng/ml of LIF (Chemicon), 10% FCS (ES qualified; Gibco, Grand Island, NY), or 300 ng/ml Noggin (R&D Systems), respectively, along with BMP4.

Flow cytometry. Flow cytometry was performed with EPICS ALTRA system (Beckman Coulter) as described previously (Furue et al. 2005; Hayashi et al. 2007). In this study, goat anti-Cdh3 antibody (R&D systems) was visualized with AlexaFluor-488-conjugated mouse antigoat IgG (Invitrogen, Carlsbad, CA). For DNA content analysis, ethanol-fixed samples were stained with propidium iodide (PI).

Immunocytochemistry. Immunocytochemistry was performed as described previously (Furue et al. 2005; Hayashi et al. 2007). Briefly, mESCs were fixed in 4% (*w/v*) paraformaldehyde or ice-cold acetone, permeabilized with 0.1% Triton X-100, and reacted with primary antibodies. The primary antibodies were visualized with AlexaFluor-488-conjugated antirabbit, antimouse, or antigoat IgG or AlexaFluor-594-conjugated donkey antimouse, antirabbit, or antigoat IgG (Invitrogen). The primary antibodies used are as follows: anti-Cdx2 antibody (Biogenex, San Ramon, CA; 1:100), anti-Cdh3 antibody (R&D systems; 1:200), anti-CK7 antibody (Chemicon; 1:100), anti-Cx31 antibody (Chemicon; 1:100), anti-Nanog antibody (ReproCell, Tokyo, Japan; 1:200), and anti-SSEA1 antibody (Kyowa, Tokyo, Japan; 1:100).

Transfection. mESCs were seeded at a density of 5×10^5 cells per well in a six-well plate coated with type I collagen in ESF7. The mESCs were transfected with plasmid DNA

using Lipofectamine 2000 (Invitrogen), according to the supplier's instructions. For inhibitory Smad overexpression experiment, Smad6 expression vector comprising whole Smad6 cDNA under CAG promoter in pCAG-IRES-PURO plasmid (a gift of Dr. Imamura) was used. The pCAG-IRES-PURO-FLAG was used as a mock. Transfected cells were reseeded in ESF5 with 10 ng/ml of BMP4 and 1 μg/ml of Puromycin, 24 h after transfection. These cells were used for immunocytochemistry and reverse transcription–polymerase chain reaction (RT–PCR), 96 h after transfection. For *Cdx2*-knockdown experiment, the shRNA for *Cdx2* expression vector consisted of 29-mer shRNA constructs against Mouse *Cdx2* under U6 promoter in pRS plasmid (purchased from OriGene, Rockville, MD). The pRS plasmid was used as a mock. Transfected cells were reseeded in ESF7 with 0.5 μg/ml of Puromycin, 24 h after transfection. After two passages on this culture conditions, these cells were used for immunofluorescence detection and RT–PCR.

Chromatin immunoprecipitation assay. For chromatin immunoprecipitation (ChIP) assay of endogenous proteins, the mESCs (D3 line) were cultured in ESF5 medium for 48 h on laminin and treated with 100 ng/ml of BMP4 for 1 h. The cells were cross-linked with 1% formaldehyde for 10 min at 37°C. To stop the cross-linking, the samples were washed twice with ice-cold phosphate-buffered saline (PBS) with complete protease inhibitors mixture (Roche). After gentle washing with ChIP lysis buffer [1% sodium dodecyl sulfate (SDS), 10 mM EDTA, 50 mM Tris–HCl (pH 8.0), complete protease inhibitor mixture], the samples were lysed with 200 μl of ChIP lysis buffer. The lysates were then mixed with 800 μl of ChIP dilution buffer [0.01% SDS, 1.1% Triton X-100, 1.2 mM EDTA, 16.7 mM Tris–HCl (pH 8.0), 167 mM NaCl, complete protease inhibitor mixture] and sonicated four times for 10 s each at the maximum setting (Sonifier 150; Branson, Danbury, CT). Then, 1 ml of ChIP dilution buffer was added, and the samples were centrifuged at 17,000×*g* for 10 min. The supernatants were transferred to a fresh centrifuge tube. An aliquot of 200 μl of the supernatant was stored at 4°C as the input DNA sample. These supernatants were conjugated with anti-phospho Smad1/5/8 antibody (Chemicon) or goat normal IgG (Upstate Biotechnology) bound with Dynabeads Protein G (Invitrogen) through overnight incubation at 4°C with rotation. These antibodies were found to adhere to the Dynabeads Protein G when 5 μg of the antibodies was incubated in 0.1 mg/ml of BSA in PBS for 1 h at room temperature with rotation. The beads were collected with Dynal MPC-S (Invitrogen) and were washed sequentially for 5 min each in low-salt buffer [0.1% SDS, 1% Triton X-100, 2 mM EDTA, 20 mM Tris–HCl (pH 8.0), 150 mM NaCl], high-salt buffer [0.1% SDS, 1% Triton X-100, 2 mM EDTA, 20 mM Tris–HCl (pH 8.0), 500 mM NaCl], and LiCl buffer [0.25 M LiCl, 1% Nonidet P-40, 1% deoxycholic acid, 1 mM EDTA, 10 mM Tris–HCl (pH 8.0)]. The precipitates were then washed twice with ChIP TE buffer [10 mM Tris–HCl (pH 8.0), 1 mM EDTA] for 5 min. The immunocomplex was extracted twice by incubation for 30 min at room temperature with 200 μl of ChIP elution buffer (1% SDS, 0.1 M $NaHCO_3$, 10 mM DTT). The eluates and input DNA solutions were supplemented with 5 M NaCl to a final concentration of 200 mM and heated at 65°C for 8–12 h to reverse the formaldehyde cross-linking. All the samples were sequentially treated for 30 min with RNase I (Wako) at 37°C and for 1 h with proteinase K (Takara Bio) at 55°C. The DNA fragments were purified using the QIAquick PCR purification Kit (Qiagen, Hilden, Germany) and analyzed by PCR. The primers, annealing temperature, and number of cycles in the PCR analysis are as follows: for *Cdx2* Intronic Conserved Sequence 1 (CICS1), forward, 5′-GGGCCA CAGCTTCCCTACAT-3′ and reverse, 5′-TGGGTGGTCCGA GACTAGGG-3′, 60°C, 31 cycles; for DS 4 kb, forward, 5′-ATGCCAGAGCCAACCTGGAC-3′ and reverse, 5′-CTCCCGACTTCCCTTCACCA-3′, 60°C, 32 cycles; and for US 4 kb, forward, 5′-AGCCAAG GACCCTTGTTGCT-3′ and reverse, 5′–GGGGACTTGAA CACCCTTCC-3′, 60°C, 32 cycles.

Electrophoretic mobility shift assay. The proteins used in the electrophoretic mobility shift assay (EMSA) were transcribed and translated from the expression vectors pCS2-GST-Smad1 and pCS2-GST-Smad4 in BL21 *E. coli* strain. The probes generated from the sense and the antisense oligonucleotides were labeled with Cy5.5 (Sigma-Aldrich), mixed, and annealed. The DNA–protein binding reaction was performed in the binding buffer [20 mM HEPES (pH 7.8), 45 mM KCl, 10 mM NaCl, 1 mM EDTA, 10% (vol/vol) glycerol, 0.1% Nonidet P-40, 0.2 mg/ml BSA, 1 mM DTT] at 4°C for 1 h. After electrophoresis, the binding reactions were analyzed by using the Odyssey image reader (Li-Cor, Lincoln, NE; ALOKA, Tokyo, Japan) for the Cy5.5-labeled probe. The sense strand sequences of the probes used in EMSA are as follows: 5′-ACAAGGGCGCCCGGCGCCGACAGCGG TCTTGCCACCTCGGCGCGGGACTT-3 ′.

Luciferase assay. The pGL4.74 (Promega) plasmid was used as an internal control. Cultured cells were transfected with the reporter vectors (pGL4.23 with Cdx2-intron1 firefly, 4 μg; Renilla, 100 ng) and were harvested 48 h after transfection. Reporter activities were measured by using the dual-luciferase reporter assay system (Promega). Each assay was performed in duplicate, and all the results presented the mean values (n=4).

RT–PCR. RT–PCR was performed as described previously (Furue et al. 2005; Hayashi et al. 2007). Briefly, total RNA

was extracted from the cultured cells using the total RNA extraction kit (Agilent, Wilmington, DE) and reverse-transcribed using Quantitect RT kit (Qiagen). Quantitative real-time PCR was performed with SYBR Green PCR Master Mix according to the supplier's directions (Applied Biosystems, Foster City, CA) in ABI PRISM 7700 sequence detector or Step One Plus sequence detector (Applied Biosystems). Relative expression of mRNA was calculated and compared with the expression in mouse whole-day 10.5 embryos or 12.5 placenta. Conventional PCR for the detection of trophoblast marker expression or ChIP assay was performed with SYBR Green PCR Master Mix according to the supplier's directions. The sequences of the primers are listed in the Table 1. All the results are given as the mean values (n=4).

Western blot. Western blot was performed as described previously (Furue et al. 2005; Hayashi et al. 2007). Briefly, to detect the phosphorylation of Smads, mESCs were seeded at a density of 6×10^5 cells per square centimeter on six-well plates in the ESF basal medium and were stimulated using 100 ng/ml of BMP4 for 0, 15, or 60 min. The cells were lysed in 200 μl of ice-cold lysis buffer (50 mM Tris–HCl (pH 7.4), 150 mM NaCl, 0.1% SDS, 1 mM Na_3Vo_4, 0.5% sodium deoxycholate, 5 mM EDTA, 1% NP-40) and 250 μl of PBS. Protein samples (25 or 50 μg) were separated in a 12.5% SDS–polyacrylamide gel and electroblotted to a polyvinylidene fluoride membrane (Amersham, Piscataway, NJ). After incubating in the blocking buffer for 30 min at room temperature, the membrane was incubated with primary antibodies overnight at 4°C. The primary antibodies used are as follows: anti-α-tubulin (Sigma, 1:1,000), anti-Smad1/5/8 (Santa Cruz Biotechnology, Santa Cruz, CA, 1:1,000), anti-phospho Smad1/5/8 (Cell Signaling Technology, Beverly, MA, 1:1,000), and anti-Smad6 (Abcam, Cambridge, UK, 1:1,000). The membranes were then reacted with secondary antibodies followed by horseradish peroxidase substrate, according to the supplier's protocol (Pierce Biotechnology, Rockford, IL). Protein bands on the membranes were visualized with LAS-1000 and PRO-LAS 1000 software (Fujifilm, Tokyo, Japan).

Results

The characterization of BMP4-treated cells in defined conditions. We observed morphological changes of the cells when undifferentiated mES cells at a density of 5×10^3 cells per square centimeter were cultured in ESF5 medium supplemented with 10 ng/ml BMP4 on laminin-coated dishes for 4 d. The morphology of the majority of cells became cobblestone-shaped (Fig. 1*A*, left). Before the cells reached to confluent, we subcultured the cells into the same culture conditions at a density of 2×10^4 cells per square centimeter on culture day 4. After four additional days in culture, multinuclear cells appeared (Fig. 1*A*, right). Trophoblast stem cells (TSCs) exhibit a cobblestone morphology (Tanaka et al. 1998) and subsequently differentiate into multinuclear trophoblast (Simmons and Cross 2005). These findings suggested the possibility that mESCs cultured with BMP4 in ESF5 might differentiate into trophoblast lineages. To explore this possibility further, we examined the gene expression of transcription factors which are expressed in trophoblast, *Cdx2* (Strumpf et al. 2005), *Dlx3* (Morasso et al. 1999), *Eomes* (Russ et al. 2000), *Errb* (Luo et al. 1997), *Esx1* (Li and Behringer 1998), *Ets2* (Yamamoto et al. 1998), *Gata3* (Ng et al. 1994), *Hand1* (Cross et al. 1995), *Mash2* (Guillemot et al. 1995), and *Psx1* (Chun et al. 1999) in the differentiated cells by quantitative real-time RT–PCR. The relative mRNA levels of the majority of these transcription factors were increased over tenfold compared with those of the undifferentiated mESCs (Fig. 1*B*). The mRNA levels of *Eomes*, *Errb*, and *Ets2*, which were involved in self-renewal of undifferentiated TSCs (Luo et al. 1997; Russ et al. 2000; Wen et al. 2007), were not increased. To confirm whether BMP4 specifically activates the expression of trophoblast markers, we examined the transcription of other cell lineage markers in early mammalian development, *Sox1* (ectoderm), *Flk1* (mesoderm), *Mixl1* (definitive endoderm), and *Gata6* (primitive extraembryonic endoderm) in the cells cultured with BMP4 in ESF5 medium on culture day 4 by quantitative real-time RT–PCR. The gene expression of the ectoderm, mesoderm, definitive endoderm, or extraembryonic endoderm cell lineage markers examined here was no higher than that in undifferentiated mESCs (Fig. 1*C*). These results indicate that the differentiated cells specifically upregulated transcription factors for trophoblast.

As the mESCs proliferated in a dose-dependent manner in response to BMP4 concentration in ESF5 medium (Fig. 1*D*) and did not proliferate without addition of BMP4, we could not compare the gene expression with those in the BMP4-untreated cells. To examine whether these genes were specifically induced in BMP4-treated cells or not, we compared the effect of FGF4 or activin with that of BMP4 on mESC gene expression. Gene expression profiles in the cells cultured with BMP4, activin, or FGF4 in ESF5 on laminin for 4 d were analyzed by quantitative RT–PCR. FGF-4 increased the *Cdx2* expression in the cells as BMP4 did, but activin did not increase *Cdx2* expression. Neither FGF-4 nor activin increased the expression of *Dlx3*, *Esx1*, *Gata3*, *Hand1*, *Mash2*, or *Psx1* (Fig. 1*E*). These results indicated that BMP4 specifically upregulated the expression of these trophoblast-specific transcription factors.

Table 1. Primer pairs used in RT–PCR

Names	Sequences	Product size	Cycles
Cdx2	5′-CTGCTGTAGGCGGAATGTATGTCT-3′ 5′-AAGGCTTGTTTGGCTCGTTACAC-3′	146	–
Dlx3	5′-TACTCGCCCAAGTCGGAATA-3′ 5′-AGTAGATCGTTCGCGGCTTT-3′	174	–
Eomes	5′-CGGCAAAGCGGACAATAACA-3′ 5′-ATGTGCAGCCTCGGTTGGTA-3′	195	–
Errb	5′-GCTGTATGCTATGCCTCCCAACG-3′ 5′-ACTCTGCAGCAGGCTCATCTGGT-3′	166	–
Esx1	5′-GAGCTGGAGGCCTTTTTCCA-3′ 5′-ACACCCACAGGGGGACTCAT-3′	194	–
Ets2	5′-CTCGGCTCAACACCGTCAAT-3′ 5′-AGCTGTCCCCACCGTTCTCT-3′	132	–
Flk1	5′-TCCTACAGACCCGGCCAAAC-3′ 5′-ACACGTTGGCAGCTTGGATG-3′	163	–
Gapdh	5′-ACCCAGAAGACTGTGGATGG-3′ 5′-CACATTGGGGGTAGGAACAC-3′	173	–
Gata3	5′-GGGCTACGGTGCAGAGGTAT-3′ 5′-TGGATGGACGTCTTGGAGAA-3′	163	–
Gcm1	5′-TACCTGAGACCCGCCATCTG-3′ 5′-AAGATGAAGCGTCCGTCGTG-3′	152	35
Hand1	5′-TCGCCGAGCTAAATGGAGAA-3′ 5′-TGCTGAGGCAACTCCCTTTT-3′	124	–
Mash2	5′-CGGGATCTGCACTCGAGGAT-3′ 5′-GGTGGGAAGTGGACGTTTGC-3′	183	–
Mixl1	5′-AAGTTGGGGAGTACACAATG-3′ 5′-CACCATACCACACATATGGA-3′	195	–
Pl1	5′-CATTTGGCTGAACTGTCTCA-3′ 5′-GACTTCCTCTCGATTCTCTG-3′	111	35
Plf	5′-AGGAACAAGCCAGGCTCACA-3′ 5′-TTCCGGACTGCGTTGATCTT-3′	178	35
Psx1	5′-CGATGGATGGGTGTGGATGA-3′ 5′-TGACAGGGCTGGCACTCAAG-3′	165	–
Sox1	5′-GTCATGTCCGAGGCCGAGAA-3′ 5′-AGCAGCGTCTTGGTCTTGCG-3′	118	–
Tpbpa	5′-AGTCCCTGAAGCGCAGTTGG-3′ 5′-TTGGAGCCTTCCGTCTCCTG-3′	138	35
Tpbpb	5′-GTCATCCTGTGCCTGGGTGT-3′ 5′-TGCCATCCTTCTCCTGGTCA-3′	163	35

To characterize these putative trophoblast cells, we further analyzed the expression of the trophoblast marker proteins Cdh3 (placental cadherin; Nose and Takeichi 1986), Cdx2, cytokeratin (CK) 7 (Lu et al. 2005), and connexin (Cx) 31 (Zheng-Fischhofer et al. 2007), by immunocytochemistry. The differentiated cells expressed Cdh3, Cdx2, CK7, and Cx31 proteins (Fig. 2*A*). Furthermore, we examined the expression of additional trophoblast-specific genes: *Gcm1* (Anson-Cartwright et al. 2000), *Placental lactogen* (*Pl*)*-1* (Faria et al. 1991), *Plf* (Simmons et al. 2008), *Tpbpa*, and *Tpbpb* (Lescisin et al. 1988) by RT–PCR. These trophoblast markers are expressed at much higher levels in placenta than in whole embryos. The expression of trophoblast marker genes was prominent in the cells cultured with BMP4 in ESF5 for 8 d (Fig. 2*B*). By flow cytometry analysis, 83.2% of cells cultured with BMP4 in ESF5 were positive for Cdh3 expression (Fig. 2*C*). These results indicate that the majority of the differentiated cells exhibit trophoblast characteristics. We observed multinuclear cells surrounded by Cdh3 in this culture conditions, which is a characteristic of differentiated trophoblast (Simmons and Cross 2005; Fig. 2*D*). To examine the frequencies of multinuclear cells in the culture, the intensity of PI in the cells cultured with BMP4 in ESF5 for 8 d was examined. A small population of hyperploid cells (>4 N) was observed in the differentiated cell cultures (Fig. 2*E*). The percentage of hyperploid cells (>4 N) was 37% in the cells, suggesting the presence of multinuclear differentiated trophoblast. We have confirmed that other mESC lines, B6G-2, E14, and EB3, also

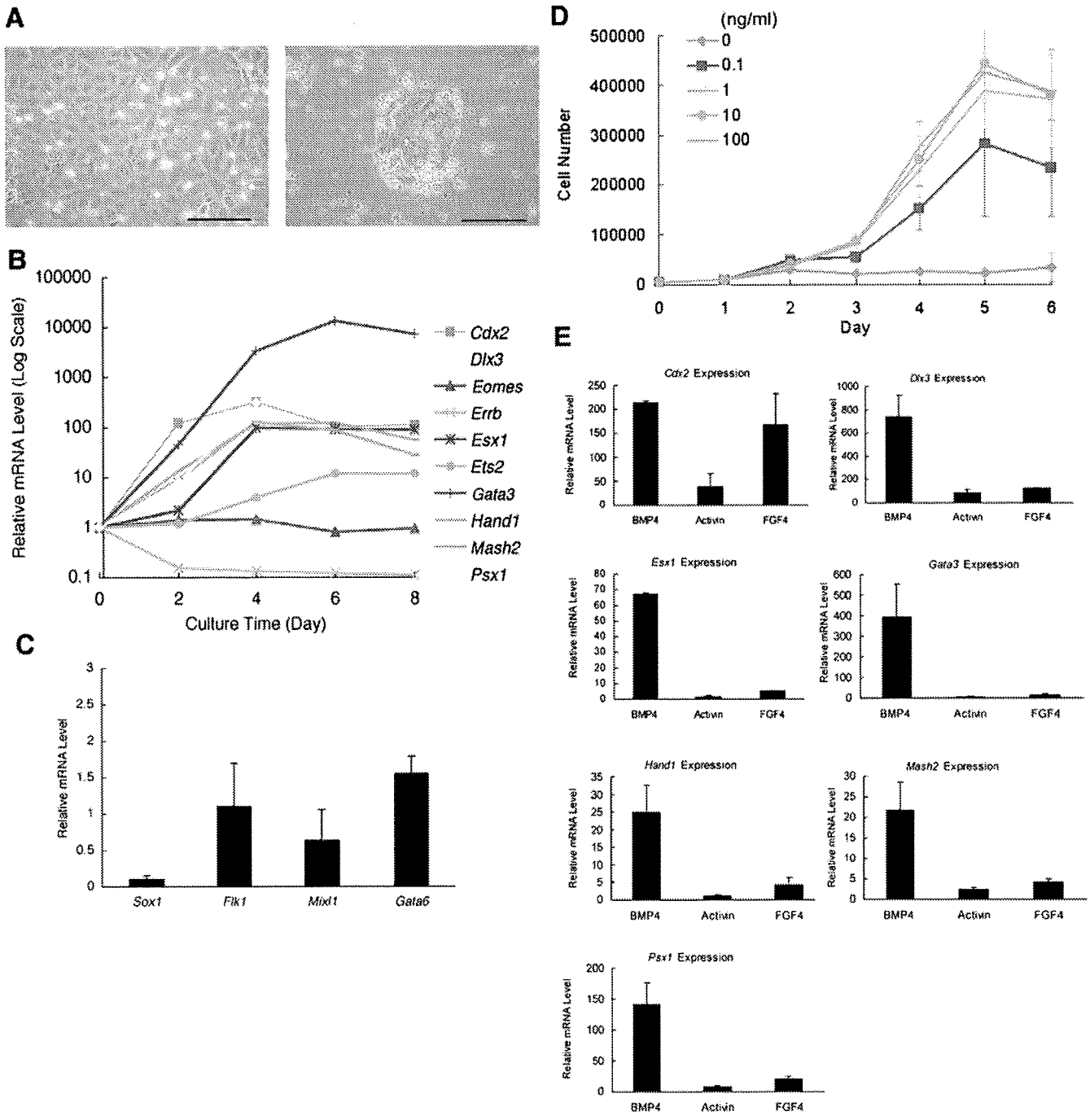

Figure 1. The effect of BMP4 on mESCs in defined culture conditions. (*A*) phase contrast photomicrographs of differentiated mESCs cultured in BMP4-supplemented ESF5 medium for 4 d (*left*) and 8 d (*right*). *Scale bars* are 100 μm. (*B*) quantitative real-time RT–PCR analysis of trophoblast-specific transcription factor expressions. The mESCs cultured in BMP4-supplemented ESF5 medium for 0, 2, 4, 6, and 8 d were analyzed. (*C*) Quantitative RT–PCR analysis of differentiation markers of mESCs. The cells cultured in BMP4-supplemented ESF5 medium for 4 d were analyzed. The amount of undifferentiated mESCs is indicated as 1. (*D*) Proliferation of differentiating mESCs on various BMP4 concentrations. mESCs were seeded in a 24-well dish at 5×10^3 cells per well on each BMP4 concentration in ESF5. Cells were counted every 24 h. The values are the mean ± SEM (n=4). (*E*) quantitative RT–PCR analysis of BMP4-induced trophoblast transcription factors in mESCs cultured in BMP4, activin A (10 ng/ml), or FGF4-supplemented (25 ng/ml) ESF5 medium on laminin for 4 d was analyzed. The gene expressions were normalized by the amount of *Gapdh*. The amount of the undifferentiated mES is indicated as 1. The values are the mean ± SEM (n=4).

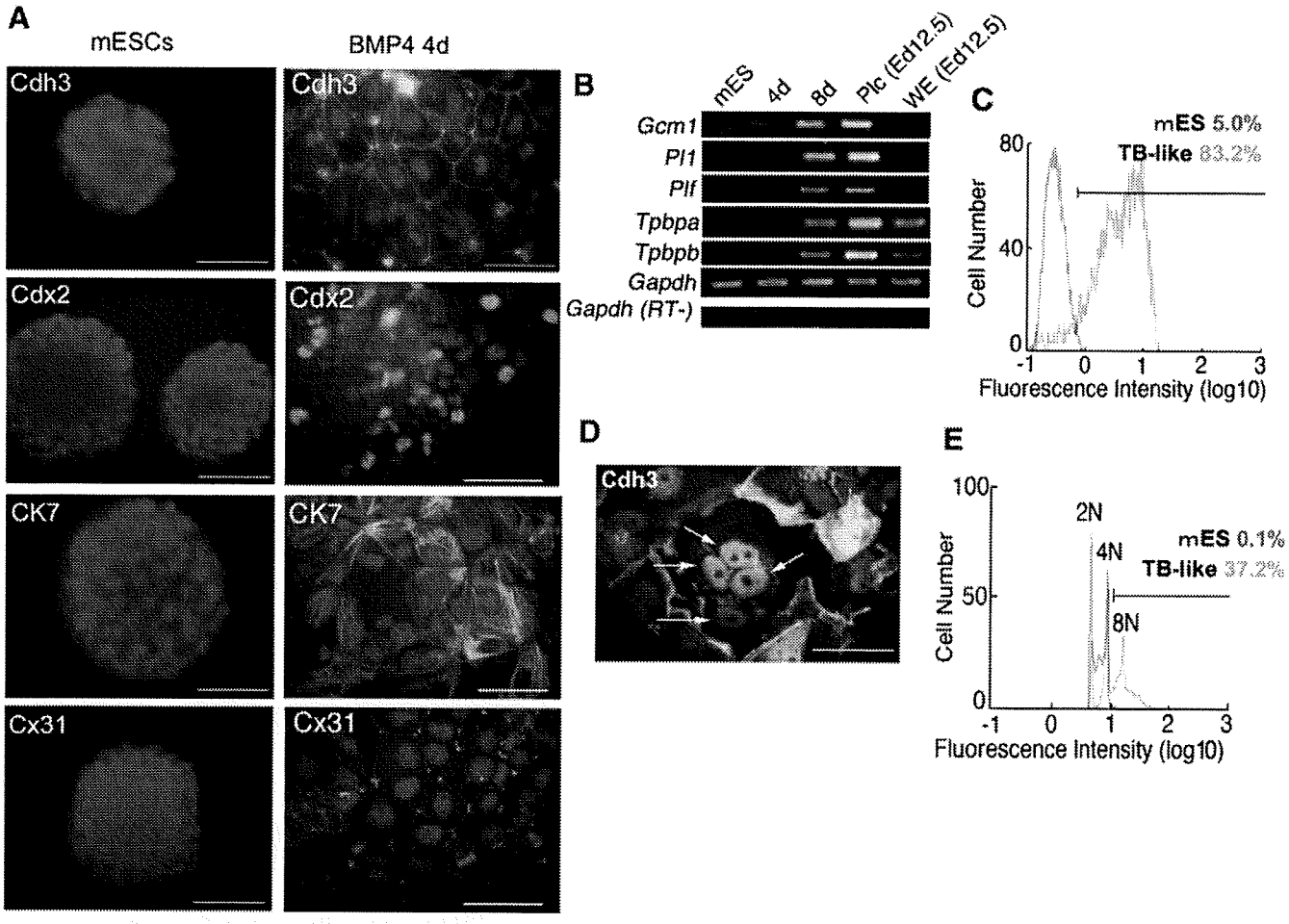

Figure 2. Differentiation into trophoblast from mESCs in vivo. (*A*) Immunocytostaining with trophoblast marker antibodies of the cells cultured in BMP4-supplemented ESF5 medium for 4 d (*right*) or undifferentiated mESCs (*left*). Immunoreactivity of Cdh3 (*upper left*), Cdx2 (*upper right*), CK7 (*lower left*), and Cx31 (*lower right*) was visualized with AlexaFluor-488-conjugated secondary antibodies (*green*). Nuclei were stained with DAPI (*blue*). *Scale bars* were 50 μm. (*B*) RT–PCR analysis of the expression of placental markers in differentiated mESCs. (*C*) Flow cytometric analysis of mESCs (*blue*) and differentiated cells at eight culture days (*red*). (*D*) Immunocytostaining with anti-Cdh3 antibodies of the cells cultured in BMP4-supplemented ESF5 medium for 8 d. *Arrows* indicate the nuclei of hyperploid cells. *Scale bars* were 50 μm. (*E*) Flow cytometric analysis of mESCs (*blue*) and differentiated cells at eight culture days (*red*). The DNA contents were visualized with propidium iodide. Diploid (2N), tetraploid (4N), and octaploid (8N) DNA contents are indicated in the DNA content graph.

differentiated into trophoblast-like cells under these conditions (data not shown).

We examined the effect of extracellular matrix on the differentiation into trophoblast cells from mESCs. We found that the cells steadily proliferated and expressed CK7 when mESC were cultured with BMP4 in ESF5 on fibronectin or laminin (Fig. 3). In contrast, the cells died and failed to express CK7 on type I collagen or PDL. These results indicate that fibronectin and laminin promoted mESC differentiation into trophoblast lineages.

The effect of serum and LIF on mESC differentiation into trophoblast cells. Although it is generally accepted that few mESCs differentiate into trophoblast lineages, we successfully directed differentiation of several mESC lines into trophoblast cells. We presume that this phenotype stems from our use of serum-free culture conditions. To elucidate the effects of serum on mESC differentiation into trophoblast, we compared trophoblast marker expression in the cells cultured with BMP4 in ESF5 medium in the presence or absence of 10% FCS. The addition of FCS decreased BMP4-induced expression of trophoblast transcription factors (Fig. 4*A*) and Cdh3 protein expression (Fig. 4*B*). These results indicate that FCS inhibited the differentiation of mESCs into trophoblast. Another candidate inhibitor of mESC differentiation into trophoblast is LIF, which is known to maintain mESCs in the undifferentiated state (Smith et al. 1988; Williams et al. 1988). To elucidate the effects of LIF on trophoblast differentiation, we examined trophoblast gene expression in cells cultured with BMP4 in the presence or absence of 10 ng/

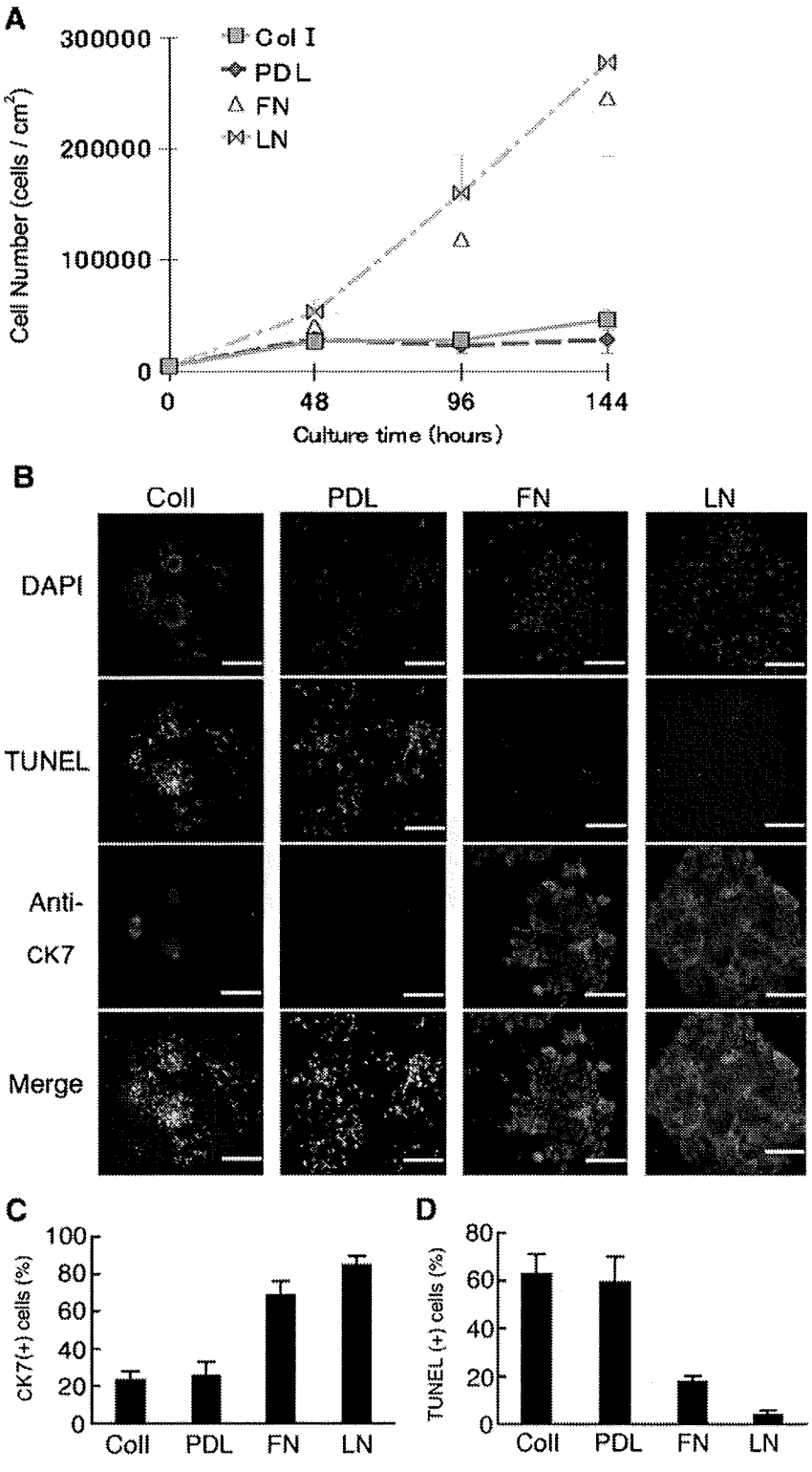

Figure 3. The effect of ECM components on the differentiation into trophoblast from mESCs. (*A*) Proliferation of differentiating mESCs on various ECM components. mESCs were seeded in a 24-well dish at 5×10^3 cells per well on each ECM component in ESF5 medium supplemented with BMP4. Cells were counted every 48 h. The values are the mean ± SEM (n=3). (*B*) Immunocytostaining and TUNEL assay of the differentiated mESCs cultured for 4 d in BMP4-supplemented medium. As trophoblast markers, CK7 was detected with specific antibodies (*red*). TUNEL assay (Chemicon) was performed according to the manufacturers' direction and labeled fixed cells with fluorescence (*green*). Nuclei were stained with DAPI (*blue*). *Scale bars* are 50 μm. (*C*) Percentages of CK7-positive cells. Percentages are calculated from the observation of more than 500 cells for each sample. The values are the mean + SEM (n=3). (*D*) Percentages of TUNEL-positive cells. Percentages are calculated from the observation of more than 500 cells for each sample. The values are the mean + SEM (n=3).

ml of LIF in ESF5. Addition of LIF decreased the BMP4-induced expression of trophoblast-specific transcription factors (Fig. 4*C*) and Cdh3 protein expression (Fig. 4*D*) and enhanced the expression of undifferentiated pluripotent stem cell markers, Nanog and SSEA1 (Fig. 4*E*). These results suggested that LIF inhibited differentiation of mESCs into trophoblast and confirmed that BMP4 in conjunction with LIF functions to maintain the undifferentiated state of mESCs.

Involvement of BMP–Smad pathway in mESC differentiation into trophoblast. To examine whether BMP4 itself may promote the differentiation of mESCs into trophoblast, we

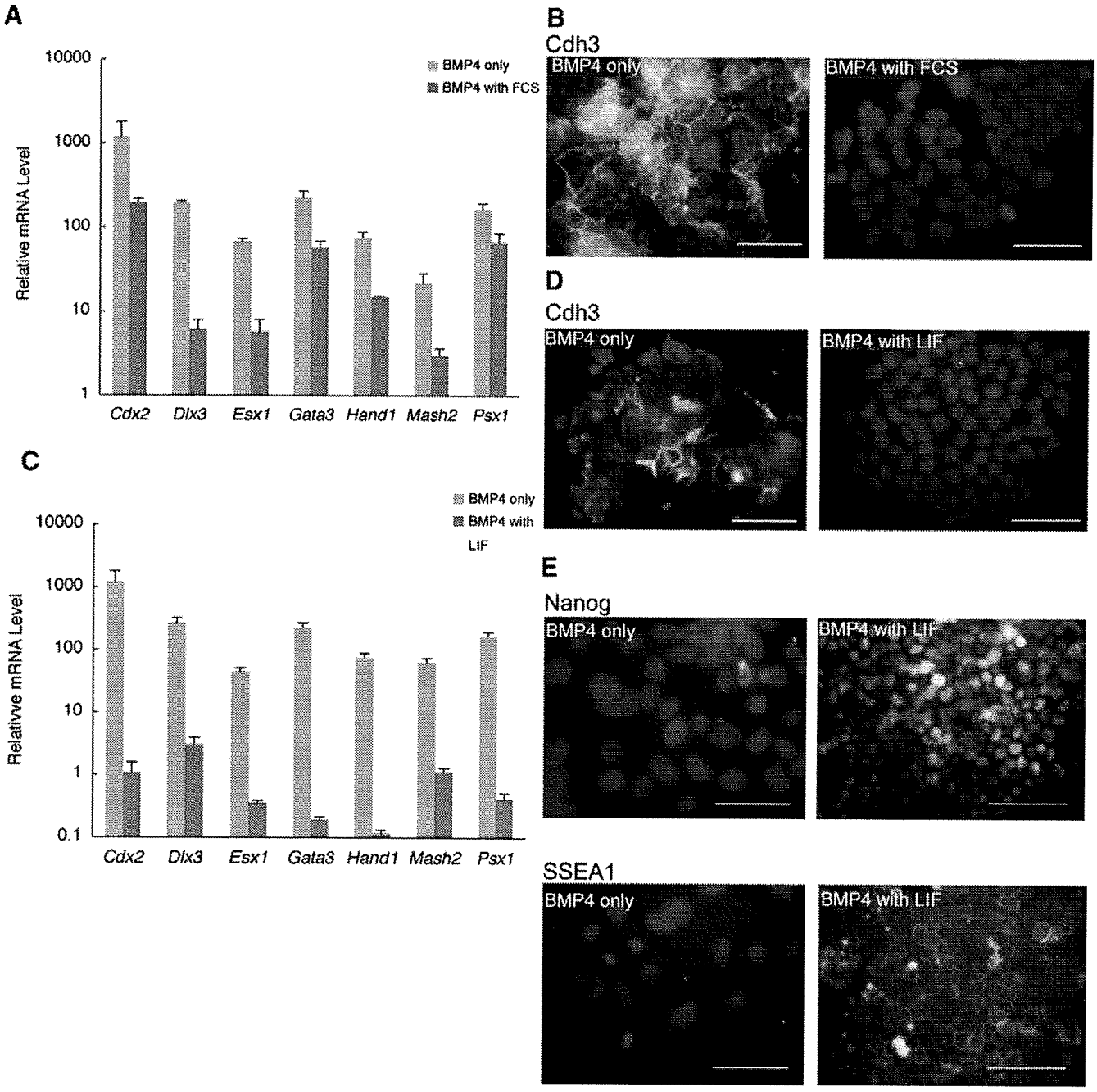

Figure 4. Effect of FCS and LIF on the differentiation into trophoblast. The effect of FCS: the cells were cultured in BMP4-supplemented ESF5 medium with 10% FCS (indicating as "BMP4 with FCS") or without FCS (indicating as "BMP4 only") for 4 d. (*A*) Quantitative real-time RT–PCR analysis of the expression of trophoblast-specific transcription factors. The gene expressions were normalized by the amount of *Gapdh*. The values are the mean ± SEM (n=4). (*B*) Immunocytochemistry with Cdh3 antibodies. Immunopositive reaction of Cdh3 antibody was visualized with AlexaFluor-488-conjugated secondary antibodies (*green*). Nuclei were stained with DAPI (*blue*). *Scale bars* are 50 μm. The effect of LIF: the cells were cultured in BMP4-supplemented ESF5 medium with 10 ng/ml of LIF (indicating as "BMP4 with LIF") or without LIF (indicating as "BMP4 only") for 4 d. (*C*) Quantitative real-time RT–PCR analysis of the expression of trophoblast-specific transcription factors. (*D*) Immunocytochemistry with Cdh3 antibodies. (*E*) Immunocytochemistry with anti-Nanog or anti-SSEA1 antibodies. Immunopositive reaction of anti-Nanog or anti-SSEA1 antibody was visualized with AlexaFluor-488-conjugated secondary antibodies (*green*).

tested the effects of a BMP antagonist, Noggin (300 ng/ml), on the response of mESCs to BMP4. Addition of Noggin decreased the BMP4-induced expression of trophoblast transcription factors (Fig. 5*A*) as well as Cdh3 (Fig. 5*B*) in the differentiated cells. This result indicated that BMP4 itself promoted the mESC differentiation into trophoblast. Next, we examined whether the BMP–Smad pathway was involved in the BMP4-induced differentiation of

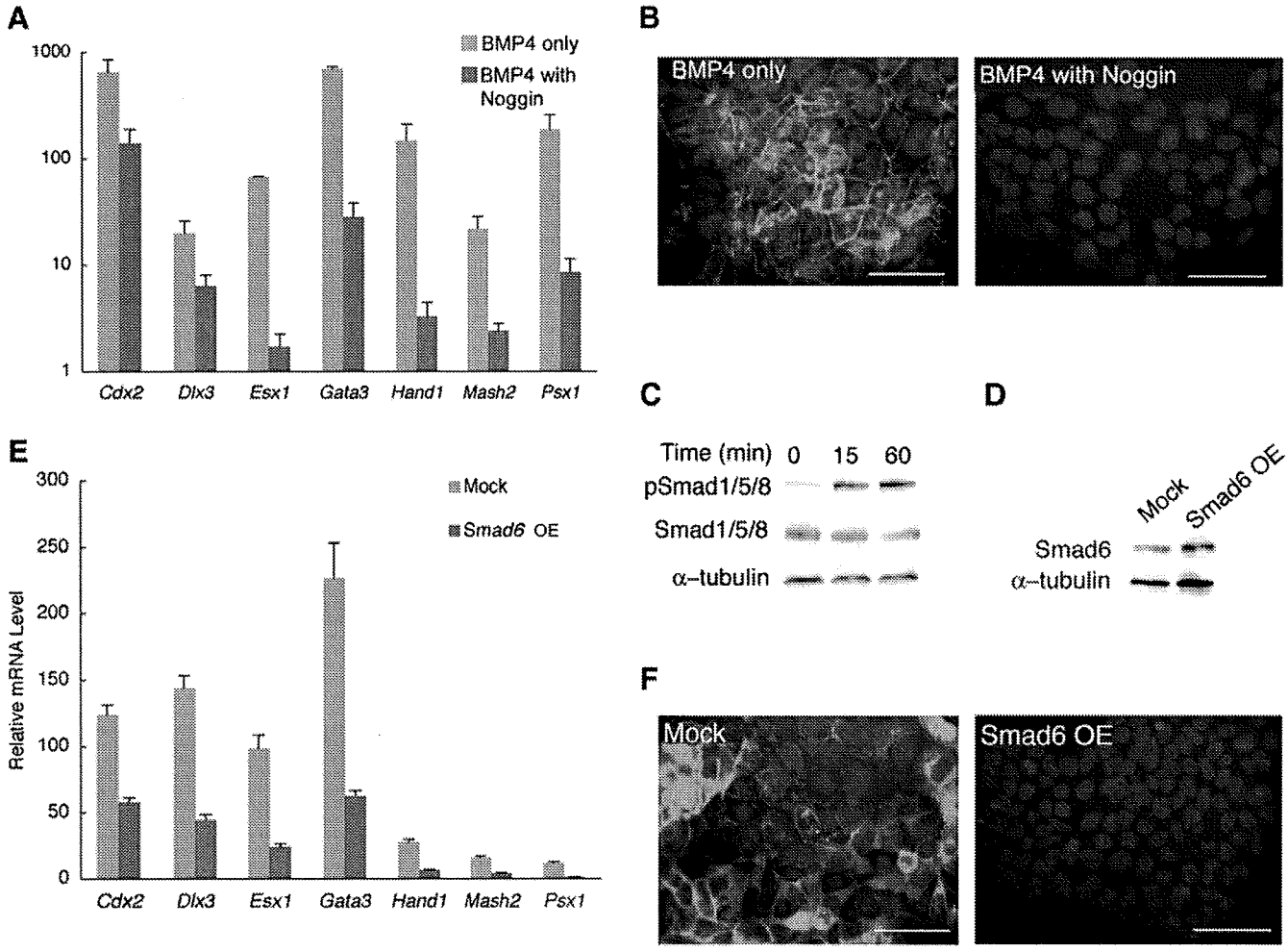

Figure 5. The effects of Noggin, inhibitory Smad6 on the BMP4-induced differentiation of mESCs into trophoblast. The effect of Noggin: the cells were cultured in BMP4-supplemented ESF5 medium with 300 ng/ml of Noggin (indicating as "BMP4 with Noggin") or without Noggin (indicating as "BMP4 only") for 4 d. (*A*) Quantitative real-time RT–PCR analysis of the BMP4-induced expression of trophoblast-specific transcription factors. These gene expressions were normalized by the amount of *Gapdh*. The values are the mean ± SEM (n=4). (*B*) Immunocytostaining with Cdh3 antibodies. Immunoreactivity of Cdh3 antibody was visualized with AlexaFluor-488-conjugated secondary antibodies (*green*). Nuclei were stained with DAPI (*blue*). *Scale bars* were 50 μm. The effect of inhibitory Smad; (*C*) protein samples were lysed from the mESCs stimulated by 100 ng/ml of BMP4 for 0, 15, and 60 min. Phosphorylation level of Smad1/5/8 in mESCs was analyzed by Western blotting using antibodies to phospho Smad1/5/8 proteins or total Smad1/5/8 proteins. Alpha-tubulin was used as the loading control. (*D*) Protein samples were lysed from mESCs transfected with Smad6 plasmids (indicating as "Smad6 OE") or mock plasmids (indicating as "Mock") for 48 h. Protein content of Smad6 in mESCs was analyzed by Western blotting using antibodies to Smad6 proteins. Alpha-tubulin was used as the loading control. (*E*) The cells transfected with Smad6-expressing vectors (indicating as "Smad6 OE") or mock vectors (indicating as "Mock") were cultured in BMP4-supplemented ESF5 medium for 72 h. Quantitative real-time RT–PCR analysis of the BMP4-induced expression of trophoblast-specific transcription factors. (*F*) Immunocytostaining with Cdh3 antibodies.

mESCs into trophoblast. Western blotting analysis showed that the activation by phosphorylation of Smad1/5/8 was observed in cells treated with BMP4 (Fig. 5*C*). Furthermore, the overexpression of Smad6 (Fig. 5*D*), which inhibits the transcriptional activity of Smad proteins, decreased the BMP4-induced expression of trophoblast transcription factors (Fig. 5*E*) as well as Cdh3 (Fig. 5*F*) in the differentiated cells. These results indicated that BMP4-stimulated differentiation of mESCs into trophoblast is mediated through by the Smad pathway.

Identification of Cdx2 as a critical and direct target of BMP–Smad pathway in mESC differentiation into trophoblast. Next, we searched for a crucial gene involved in trophoblast differentiation induced by BMP4. Previous studies have demonstrated that *Cdx2* regulates the induction of trophoblast from mESCs (Niwa et al. 2005; Tolkunova et al. 2006). Thus, we hypothesized that *Cdx2* could be a crucial gene involved in trophoblast differentiation by BMP4. We generated *Cdx2*-knockdown mESCs carrying an shRNA plasmid against *Cdx2* with a puromycin-

resistance gene. The expression of *Esx1* and *Psx1* (Fig. 6*A*) and the expression of Cdh3 protein were decreased in the *Cdx2*-knockdown mESCs cultured with BMP4 in ESF5 (Fig. 6*B*). These results suggested that *Cdx2* was crucial for the BMP4-induced differentiation of mESCs into trophoblast through the regulation of the expression of *Esx1* and *Psx1*.

Finally, we explored the possibility that BMP–Smad pathway could directly regulate the *Cdx2* transcription. We first searched for the putative Smad1/5/8-binding sequence (GCCG) in the noncoding conserved sequences in the genomic region of *Cdx2* using the Vista comparative genomics tool (Frazer et al. 2004; Danno et al. 2008). We found a set of putative Smad1-binding sequences (GCCG) highly conserved among mammals in intron 1 of the *Cdx2* gene, designated as CICS1 (Fig. 7*A*). We cloned a 350-bp sequence containing CICS1 and inserted it into the pGL4.23 luciferase reporter plasmid. To confirm that this sequence has enhancer activity in response to BMP4, a luciferase reporter assay was performed in mESCs transfected with the reporter plasmid or empty plasmid. Transcriptional activity was increased in a BMP4 dose-dependent manner in transfected mESCs, whereas Noggin (300 ng/ml) decreased BMP4-induced transcriptional activity (Fig. 7*B*). These results indicate that CICS1 has BMP4-dependent transcriptional activity. To examine whether Smad proteins can bind to CICS1, we performed EMSA. EMSA revealed that the Smad proteins were bound to CICS1 in vitro (Fig. 7*C*). To confirm whether endogenous Smad proteins were bound to CICS1 in the BMP4-induced trophoblast cells, we performed ChIP assays (Fig. 7*D*, *E*). The CICS1 sequence was specifically contained in the DNA–protein complex immunoprecipitated by the anti-pSmad1 antibodies. These results demonstrate specific binding of the Smad1 proteins to CICS1 in BMP4-treated mESCs. Based on the experimental results obtained here, we conclude that *Cdx2* transcription is directly regulated by the BMP–Smad pathway during BMP4-induced mESC differentiation.

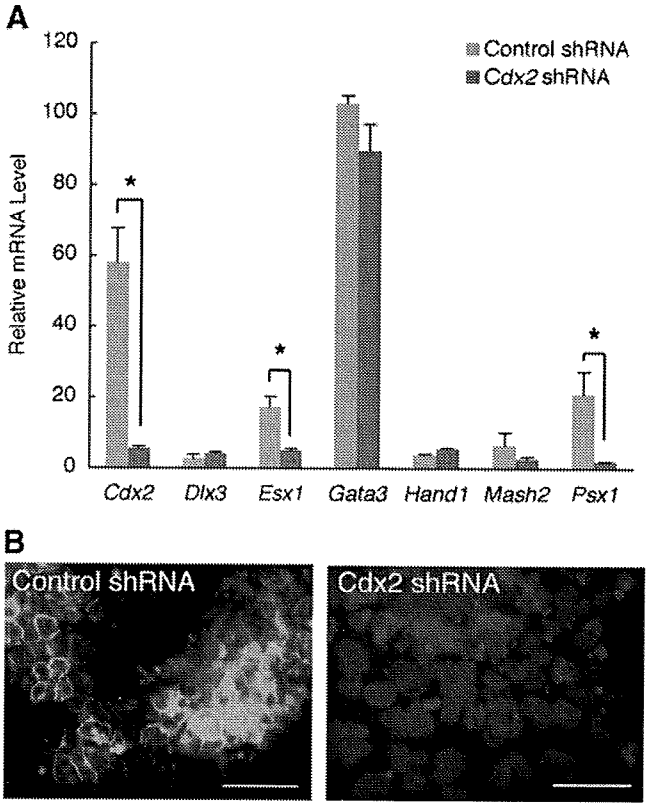

Figure 6. The effects of shRNA against *Cdx2* on the BMP4-induced differentiation of mESCs into trophoblast. The cells carrying shRNA-expressing vectors against *Cdx2* (indicating as "*Cdx2* shRNA") or control shRNA-expressing vectors (indicating as "Control shRNA") were cultured in BMP4-supplemented ESF5 medium for 48 h. (*A*) Quantitative real-time RT–PCR analysis of the BMP4-induced expression of trophoblast-specific transcription factors. These gene expressions were normalized by the amount of *Gapdh*. The values are the mean ± SEM (n=4). *Asterisks* indicate $p<0.05$ by Student's t test. (*B*) Immunocytostaining with Cdh3 antibodies. Immunoreactivity of Cdh3 antibody was visualized with AlexaFluor-488-conjugated secondary antibodies (*green*). Nuclei were stained with DAPI (*blue*). *Scale bars* were 50 μm.

Discussion

Previous studies reported that isolated ICM could partially differentiate into trophoblast (Handyside 1978; Hogan and Tilly 1978) whereas it was reported that mESCs did not contribute to extraembryonic trophoblast in chimeric embryos (Beddington and Robertson 1989). From these findings, we inferred that mESCs under certain conditions have the potential to differentiate into trophoblast lineages as well as all three embryonic germ layers. Toumadje et al. observed spontaneous expression of the trophoblast marker cytokeratin endo-A (CK8) in D3 mESC embryoid bodies cultured in serum in the absence of LIF (Toumadje et al. 2003). A recent study reported that a small subset of trophoblast-like cells appeared when mESCs were cultured on type IV collagen (Schenke-Layland et al. 2007). Another study reported that the addition of Wnt3a induced a small subset of trophoblast lineages from mESCs (He et al. 2008). These findings suggested that mESCs may have the potential to differentiate into trophoblast lineages and that the modulation of culture conditions regulates mESCs to differentiate into trophoblast in vitro.

To induce trophoblast from mESCs, laminin proved to be a key component. We previously reported that laminin or fibronectin promotes cell differentiation in our defined culture conditions (Hayashi et al. 2007). The results in this study indicated that mESC differentiated into trophoblast